Quasi Second-Order Stochastic Dominance Model for Balancing Wildfire Risks and Power Outages due to Proactive Public Safety De-Energizations

Jinshun Su, *Graduate Student Member, IEEE*, Saharnaz Mehrani, Payman Dehghanian, *Senior Member, IEEE*, and Miguel A. Lejeune

***Abstract*—Faults on overhead power line infrastructures in electric power distribution systems (DSs) can potentially ignite catastrophic wildfires, especially in areas exposed to high wind regimes, low humidity, and dense vegetation. The common practice adopted by electric utilities to build resilience against such *electrically-induced wildfires* is called public-safety power-shutoff (PSPS): strategies to intentionally and proactively de-energize power line infrastructures to prevent wildfire risks. Using a quasi second-order stochastic dominance (Q-SSD) measure, this article proposes an optimization model to generate an optimal PSPS plan which mitigates the risk of costly wildfires while keeping the intentional power outages minimal. This objective is achieved by the strategic deployment of transportable energy backup technologies in the DS, i.e., mobile power sources (MPSs). The proposed model is a stochastic mixed-integer nonlinear programming (S-MINLP) capturing the uncertainties in wildfire consequences under different weather realizations. We derive a tractable linearization procedure to reformulate the S-MINLP model as an equivalent mixed-integer linear problem. Numerical studies on the IEEE 33-node test system demonstrate the efficiency of the resulting PSPS actions in balancing the wildfire risks and the power outage consequences, and highlight the promising performance of the proposed modeling approach compared to the state-of-the-art and benchmark formulations.**

***Index Terms*—Mobile power sources (MPS), proactive de-energization, power outages, public-safety power-shutoff (PSPS), quasi second-order stochastic dominance (Q-SSD), wildfire.**

NOMENCLATURE

A. Sets

$\mathbf{I}$	Set of nodes in the distribution system (DS).
$\mathbf{L}$	Set of overhead lines in the DS.
$\mathbf{T}$	Set of periods in the decision-making horizon.
$\mathbf{S}$	Set of wildfire scenarios.
$\mathbf{M}$	Set of mobile power sources (MPSs).
$\mathbf{N}$	Set of substations in the DS.
$\mathbf{I}^m \subseteq \mathbf{I}$	Subset of candidate nodes connected to MPSs.
$\mathbf{I}' \subseteq \mathbf{I}$	Subset of nodes for MPSs initial positioning.
$\mathbf{M}^g \subseteq \mathbf{M}$	Subset of mobile energy generators (MEGs).
$\mathbf{M}^e \subseteq \mathbf{M}$	Subset of mobile energy storage systems (MESSs).
$\mathbf{N}_i \subseteq \mathbf{N}$	Subset of substations connected to node i.

B. Parameters and Constants

$D^{\Gamma}_{it}, D^{\Lambda}_{it}$	Amount of real/reactive power demand at node i at period t in DS [kW, kVar].
β_t	Price of undelivered energy from the electric utility at period t [$/kW].
γ_i	Interrupted energy assessment rate for node i [$/kW].
δ^g_m, δ^e_m	Operating cost coefficients of MPS m [$/kW].
$F^{\Gamma}_l, F^{\Lambda}_l$	Real/Reactive power capacity of overhead line l [kW, kVar].
M^v	Constant denoting the maximum value of the difference in the squared voltage magnitudes.
R_l, X_l	Resistance/Reactance of overhead line l [Ω].
$\underline{v_i}, \overline{v_i}$	Minimum/Maximum squared voltage magnitude at node i [kV^2].
$\underline{G^{\Gamma}_n}, \overline{G^{\Gamma}_n}$	Minimum/Maximum real power capacity of substation n [kW].
$\underline{G^{\Lambda}_n}, \overline{G^{\Lambda}_n}$	Minimum/Maximum reactive power capacity of substation n [kW].
T^m_{ij}	Travel time from node i to j with MPS m.
c_i	Maximum number of MPSs allowed to be connected to node i.
$\underline{A^{\Gamma}_m}, \overline{A^{\Gamma}_m}$	Minimum/Maximum real power output of MEG m [kW].
$\underline{A^{\Lambda}_m}, \overline{A^{\Lambda}_m}$	Minimum/Maximum reactive power output of MEG m [kVar].
$\varepsilon^c_m, \varepsilon^d_m$	Charging/Discharging efficiency of MESS m.
$\underline{Z_m}, \overline{Z_m}$	Minimum/Maximum state of charge of MESS m [kWh].
$\underline{J^c_m}, \overline{J^c_m}$	Minimum/Maximum charging power of MESS m [kW].

Manuscript received 2 June 2022; revised 8 April 2023; accepted 17 June 2023. Date of publication 27 June 2023; date of current version 21 February 2024. This work was supported in part by the National Science Foundation (NSF) under Grant ECCS-2114100 and Grant RISE-2220626 and in part by the Office of Naval Research (ONR) under Grant N00014-22-1-2649. Paper no. TPWRS-00794-2022. *(Corresponding author: Payman Dehghanian.)*

Jinshun Su and Payman Dehghanian are with the Department of Electrical and Computer Engineering, George Washington University, Washington, DC 20052 USA (e-mail: jsu66@gwu.edu; payman@gwu.edu).

Saharnaz Mehrani is with the Department of Information Technology and Operations Management, Florida Atlantic University, Boca Raton, FL 33431 USA (e-mail: smehrani@fau.edu).

Miguel A. Lejeune is with the Department of Decision Sciences, George Washington University, Washington, DC 20052 USA (e-mail: mlejeune @gwu.edu).

Color versions of one or more figures in this article are available at https://doi.org/10.1109/TPWRS.2023.3289788.

Digital Object Identifier 10.1109/TPWRS.2023.3289788

$\underline{J_m^d}, \overline{J_m^d}$ Minimum/Maximum discharging power of MESS m [kW].
$\underline{W_m^\Lambda}, \overline{W_m^\Lambda}$ Minimum/Maximum reactive power of MESS m [kVar].
$C^F_{\hat{L}s}$ Wildfire cost due to the ignition only on lines in set $\hat{L}$ under scenario s.

C. Decision Variables

x_{lt} Binary variable equal to 1 if overhead line l is shut-off intentionally at period t, 0 otherwise.
$\pi_{\hat{L}s}$ Binary variable equal to 1 when lines in set $\hat{L}$ are the only energized lines at the time of fault in scenario s, 0 otherwise.
μ_{imt} Binary variable equal to 1 if MPS m is connected to node i at time t, 0 otherwise.
$\kappa^c_{imt}, \kappa^d_{imt}$ Binary variable equal to 1 if MESS m is charging/dicharging at node i at time t, 0 otherwise.
C^F_s Wildfire cost under scenario s.
$y^\Gamma_{it}, y^\Lambda_{it}$ Fraction of real/reactive power outage at node i at time t.
$f^\Gamma_{lt}, f^\Lambda_{lt}$ Real/Reactive power flow in overhead line l at time t.
$\phi^\Gamma_{it}, \phi^\Lambda_{it}$ Real/Reactive power input on node i at time t.
v_{it} Squared voltage magnitude at node i at time t.
$G^\Gamma_{nt}, G^\Lambda_{nt}$ Real/Reactive power of substation n at time t.
$\psi^\Gamma_{it}, \psi^\Lambda_{it}$ Total real/reactive power injection (from all MPSs) to node i at time t.
$\varphi^\Gamma_{imt}, \varphi^\Lambda_{imt}$ Real/Reactive power output from MEG m to node i at time t.
$\omega^\Gamma_{imt}, \omega^\Lambda_{imt}$ Real/Reactive power output from MESS m to node i at time t.
Z_{mt} State of charge of MESS m at time t.
$\rho^c_{imt}, \rho^d_{imt}$ Real charging/discharging power output from MESS m to node i at time t.

I. Introduction

WILDFIRE incidents have been evidenced, in the past decade, with an increased frequency and intensity, threatening communities, disrupting social and organizational ecosystems, harming natural resources, damaging homes and structures, and taking lives [1]. In October 2017, a series of wildfires started to burn across the Wine country of Northern California, which caused insured damages exceeding $9.4 billion and the death of 44 people [2]. According to a recent report [3], in 2020, 58,950 wildfire incidents burned 10.1 million acres within the U.S., the second-most impacted acreage in a year since 1960. While wildfires could be triggered by various means, those resulting from disruptions in the electrical infrastructures are recorded as the fifth highest cause at the rate of about 8% [4]. A number of such catastrophic *electrically-induced wildfires* has been recorded in recent years in the Western United States [5], majorly due to power line faults under precarious vegetation conditions, poor line maintenance, and severe weather [6]. Most electrically-induced wildfires are directly related to power distribution systems (DSs).

Preventing wildfires is much less costly than mitigating them; a variety of long-term planning solutions — e.g., network upgrades, reinforcements and modernization, vegetation management — against the risk of electrically-induced wildfires are reviewed in [7]. The short-term (day-ahead or hours-ahead) operational practice for wildfire prevention adopted by many electric utilities is referred to as public-safety power-shutoff (PSPS): when dangerously-high winds arise, the electric utility anticipatively and intentionally pursues power line de-energization and black-outs the fire-prone areas that are home to millions of people [8]. While it has been evidenced [9] that wildfire risk could be effectively mitigated through proactive and selective power shutoffs, power line de-energization could challenge the electric power grid operation and jeopardize its performance reliability [10]. The PSPS-resulted power outages would lead to unfavorable consequences for the end-use customers. In October 2019, the intentional PSPS-caused blackouts turned off power to almost a million customers served by PG&E electric utility [11]. The economic and social impacts of a blackout on this scale, lasting for several days, are enormous with significant implications on people's health and well-being (e.g., increased mortality) [12]. The survey in [13] indicates that many Californians have experienced recent PSPS events and they—in particular health-vulnerable populations—are concerned about the resulting power outages and the impact on their daily lives [14].

Electric utilities have been exploring planning and operation solutions to address this concern. Microgrids have been found critical and effective to battle the PSPS-caused [15] and wildfire-caused [16] power outages. An optimization approach is introduced in [17] to balance PSPS consequences in power transmission systems and wildfire risk with the aim to maintain as much load delivery as possible. The authors in [18] propose a rolling horizon framework to fairly and efficiently execute PSPS decisions for mitigating wildfire ignition risk in power transmission systems. A multi-period optimization formulation is presented in [19] to optimize transmission infrastructure investments for reducing PSPS-caused power outages through the installation of grid-scale batteries and solar panels. To limit the size of PSPS-caused power outages, the authors in [20] co-optimize power line shut-offs and service restoration, where service restoration is primarily restricted to the re-energization of PSPS-caused offline power lines. The wildfire risk-aware operation planning problem in [21] aims to assist system operators in managing wildfire risks in transmission systems via enabling them to schedule an optimal PSPS action based on quantified risk values while balancing service continuity. The parent-child and iterative approaches for enforcing radiality constraints in DS are introduced in [22] to increase the efficiency of solving the PSPS problem for wildfire risk mitigation. In [23], the authors dynamically optimize the PSPS schedules for multiple days, taking into account weather uncertainties, to minimize the expected costs imposed on the electric utility. Complementing the previous studies focused on short-term PSPS operations and decision-making, authors in [24] investigate a long-term expansion planning scheme that aims to limit the wildfire ignition risk in the electric network, capturing the long-term impacts of PSPS decisions.

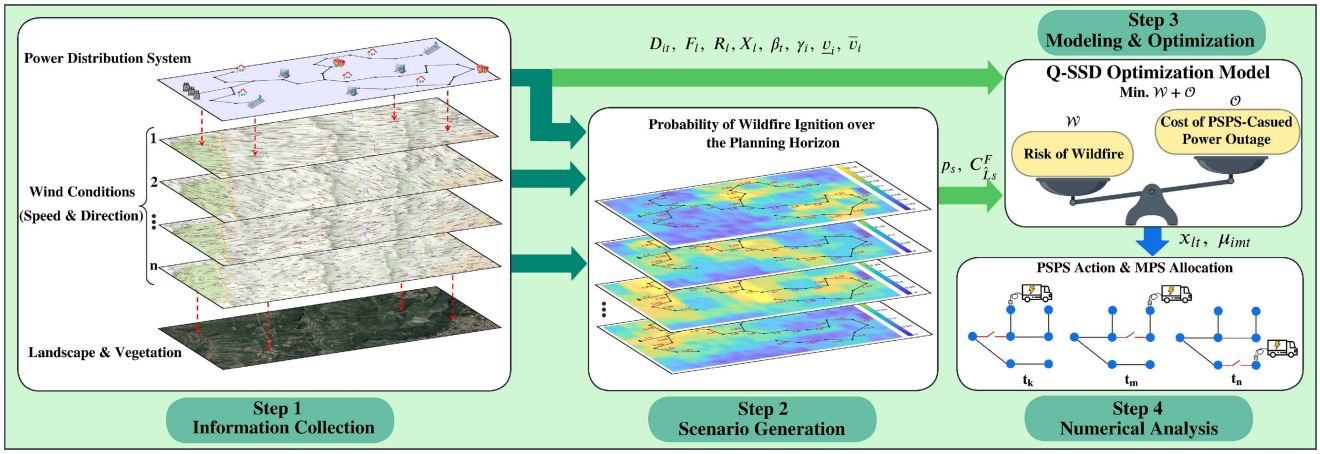

Fig. 1. Proposed quasi second-order stochastic dominance (Q-SSD) framework for balancing wildfire risk and PSPS-caused power outages.

The state-of-the-art literature [17], [18], [19], [20], [21], [22], [23] on models balancing electrically-induced wildfire risks and power outages—via offering optimal PSPS actions—has only investigated the decision-making process for selectively de-energizing power lines in the power system. However, these studies do not fully account for the simultaneous use of restoration mechanisms and power line de-energization to minimize wildfire risks while keeping the resulting power outages as minimal as possible. To develop a risk-averse model for making PSPS decisions, this article incorporates a mobility-as-a-service framework utilizing mobile power sources (MPSs) for service restoration in the DS, routing and dispatch decisions of which are jointly optimized with those of PSPS actions. MPSs including mobile emergency generators (MEGs) and mobile energy storage systems (MESSs) can be effective resources in the DS for spatio-temporal flexibility exchange during emergencies [25]. Spatio-temporal flexibility refers to the MPSs' ability to travel across space and time and deliver power to critical infrastructures and customers in need [26]. In recent years, MPSs' utilization has been widely researched to take day-ahead energy management decisions [27], and define resilience policies against emergencies [28], [29].

To the best of our knowledge, the literature lacks a framework that co-optimizes power line de-energization and MPS dispatch decisions for effective wildfire risk management in wildfire-vulnerable geographical zones. Additionally, the potential of risk-averse decision-making in the context of wildfires is yet to be fully unlocked. To fill in this knowledge gap, this article explores, for the first time, a risk-averse stochastic optimization model based on the *quasi second-order stochastic dominance* (Q-SSD) measure where decisions on the utilization of MPSs and PSPS actions to balance the risk of wildfire and the PSPS-caused power outages are made jointly. In particular,

- We present a new proactive risk-averse framework for integrated PSPS planning and MPSs dispatching decisions over a short-term horizon which accounts for undesirable weather conditions that raise the risk of electrically-induced wildfires.
- We propose a stochastic mixed-integer nonlinear programming (S-MINLP) model based on Q-SSD to mitigate the risk of wildfires while keeping the PSPS-caused power outages minimal. We develop a linearization approach to obtain a tractable mixed-integer linear program (MILP) equivalent to the S-MINLP model.
- We develop a method to generate representative wildfire risk scenarios and empirically evaluate the performance of the proposed optimization approach compared to a set of benchmark models. We numerically demonstrate the effective role of MPSs in mitigating the devastating PSPS-caused power outages.

The remainder of this article is organized as follows. In Section II, we describe the problem and the adequacy of the Q-SSD measure. We present the S-MINLP model and its reformulation method in Section III. We present the results of our experiments in Section IV and conclusions in Section V.

II. Problem Description

A. General Framework

The general idea of the proposed optimization framework is depicted in Fig. 1. In *Step 1*, we gather information on the targeted DS, weather conditions (in particular wind forecasts), the geographical landscape, and the vegetation. PG&E electric utility provides a 12-hour-ahead notification called "PSPS Warning" informing customers of an upcoming PSPS [8]. Accordingly, the proposed framework requires the prediction of wind direction and speed at least 12 hours ahead. In this study, we consider that different combinations of DS power lines provoking arc ignition would lead to wildfires of different intensities and consequences. The uncertain conditions of wind speed, humidity, and temperature result in different wildfire ignition scenarios, thereby featuring the uncertain cost of wildfires caused by different power lines. In *Step 2*, we first evaluate the probability of faults and fire ignition at each power line during the planning horizon based on the information from Step 1, and then generate possible scenarios of wildfire cost accordingly. An optimization problem based on a Q-SSD risk measure for joint decisions on PSPS

actions and the dispatch of MPSs is proposed in *Step 3* to balance wildfire risks and PSPS-caused power outages. *Step 4* provides DS operators with the optimal decisions obtained by solving the proposed proactive public safety de-energization (PPSD) problem.

B. Overview of the Q-SSD-Based Approach

Risk-averse optimization models permit to control and hedge against unfavorable outcomes based on decision-makers' risk preferences. Modeling a decision-making problem under uncertainty via *second-order stochastic dominance* (SSD) allows decision-makers to manage risk by requiring their decisions to yield a random outcome which stochastically dominates a reference random outcome. Since SSD is a well-established risk-averse and consistent risk measure, it has attracted significant attention in various contexts, such as financial portfolio selection [30], design of emergency medical service systems [31], optimal path problems [32], and operations of energy systems [33]. In order to mitigate the risk of extensive wildfires through executing PSPS actions, this study proposes a risk-averse approach based on the SSD concept. The SSD-based approach allows taking optimal PSPS decisions such that the uncertain cost of wildfires in the DS dominates a reference (or benchmark) random cost of wildfires. In this article, the dominated benchmark is designated as DS without any PSPS actions.

Since an SSD constraint is equivalent to a continuum of conditional value-at-risk (CVaR) constraints [34], we first review the concept of CVaR before presenting the specifics of our SSD-based approach. The CVaR measure [35], [36]—also known as Mean Excess, Mean Shortfall, and Tail VaR—is defined as the mean of the tail distribution exceeding the Value-at-Risk (VaR) [37]. While VaR is a percentile of loss distribution (e.g., wildfire cost distribution in this study), CVaR quantifies the *expected loss exceeding a percentile*.

Suppose that V is a random variable representing the magnitude (of the consequences) of wildfires. Let $f(\boldsymbol{x}, V)$ denote a random loss function depending on V and some controllable vector $\boldsymbol{x}$. In this study, the controllable vector includes decisions that can be taken to prevent or alleviate the impact (i.e., costs) of V (i.e., magnitude of wildfires). Let $\alpha \in (0, 1]$ be a confidence level and $VaR_\alpha(f(\boldsymbol{x}, V))$ be the value-at-risk (VaR) at the α level of the random cost function $f(\boldsymbol{x}, V)$: $VaR_\alpha = \inf\{y : \mathbb{P}(f(\boldsymbol{x}, V) \le y) \ge \alpha\}$. The CVaR of the loss function at the confidence level α, denoted $CVaR_\alpha(f(\boldsymbol{x}, V))$, is the expected value of $f(\boldsymbol{x}, V)$ exceeding $VaR_\alpha(f(\boldsymbol{x}, V))$:

$$\begin{aligned} CVaR_\alpha\left(f(\boldsymbol{x}, V)\right) &= \mathbb{E}\left[f(\boldsymbol{x}, V) | f(\boldsymbol{x}, V) \ge VaR_\alpha(f(\boldsymbol{x}, V))\right] \\ &= \min_{\eta \in \mathbb{R}} \ \eta + \frac{1}{1-\alpha}\mathbb{E}\left[(f(\boldsymbol{x}, V) - \eta)^+\right], \end{aligned} \tag{1}$$

where $(.)^+ = \max\{., 0\}$. It is known that if $VaR_\alpha(f(\boldsymbol{x}, V))$ is finite, setting η equal to $VaR_\alpha(f(\boldsymbol{x}, V))$ is optimal [35]. Therefore, in the optimal solution, we have:

$$CVaR_\alpha\left(f(\boldsymbol{x}, V)\right) = VaR_\alpha\left(f(\boldsymbol{x}, V)\right) + \frac{1}{1-\alpha}\mathbb{E}\left[(f(\boldsymbol{x}, V) - VaR_\alpha\left(f(\boldsymbol{x}, V)\right))^+\right]. \tag{2}$$

The larger the confidence level, the more risk-averse the decision-maker and the larger the CVaR.

Let $f(\boldsymbol{x}, V|\boldsymbol{x} = 0)$ denote the random loss if no PSPS action is taken (i.e., $x = 0$). The random loss $f(\boldsymbol{x}, V)$ stochastically dominates $f(\boldsymbol{x}, V|\boldsymbol{x} = 0)$ in the second-order, denoted as $f(\boldsymbol{x}, V) \succcurlyeq_{(2)} f(\boldsymbol{x}, V|\boldsymbol{x} = 0)$, if and only if the following continuum of CVaR constraints holds [30], [34]:

$$CVaR_\alpha\left(f(\boldsymbol{x}, V)\right) \le CVaR_\alpha\left(f\left(\boldsymbol{x}, V|\boldsymbol{x} = 0\right)\right) \forall \alpha \in (0, 1]. \tag{3}$$

The inequality (3) is called a CVaR-preferability constraint at confidence level α [38]. It is shown in [38] that if the random variable has a finite support, the continuum set of confidence levels can be discretized to a set of size $n - 1$ with $n < 2^{|\Omega|}$. Building upon this, we replace, in our SSD-based approach referred to as the Q-SSD-based approach, the continuum of CVaR constraints in (3) with a finite number of CVaR constraints:

$$CVaR_\alpha\left(f(\boldsymbol{x}, V)\right) \le CVaR_\alpha\left(f\left(\boldsymbol{x}, V|\boldsymbol{x} = 0\right)\right) \quad \forall \alpha \in \mathbf{A}, \tag{4}$$

where $\mathbf{A} = \{\frac{1}{n}, \ldots, \frac{n-1}{n}\}$ is a set of confidence levels (see [30] for a similar approach) and n is an arbitrary integer number. The larger n is, the closer the Q-SSD constraints (4) approximate SSD. In our Q-SSD-based approach, the objective is to find the least costly solution $\boldsymbol{x}^*$, with respect to the worst-case $CVaR_\alpha$ differential taken over all considered confidence levels $\alpha \in \mathbf{A}$. Proceeding along that way, the random loss function $f(\boldsymbol{x}^*, V)$ associated with $\boldsymbol{x}^*$ should have a right-skewed probability distribution with the probability masses concentrated on the small possible loss values. To this end, we solve the following min-max bi-level stochastic programming model for wildfire risk mitigation:

$$\min_{\boldsymbol{x} \in \mathcal{X}} \max_{\alpha \in \mathbf{A}} \left(CVaR_\alpha(f(\boldsymbol{x}, V)) - CVaR_\alpha(f(\boldsymbol{x}, V|\boldsymbol{x} = 0))\right). \tag{5}$$

In this study, we define the Q-SSD risk measure for any solution $\boldsymbol{x}$ as follows:

$$\begin{aligned} &\text{Q-SSD}(f(\boldsymbol{x}, V)) \\ &= \max_{\alpha \in \mathbf{A}} \left(CVaR_\alpha(f(\boldsymbol{x}, V)) - CVaR_\alpha(f(\boldsymbol{x}, V|\boldsymbol{x} = 0))\right). \end{aligned} \tag{6}$$

In the following two propositions, we show the relation between CVaR-preferability constraints in (4) and the optimal value of (5).

Proposition 1: If the optimal value of (5) is not positive, (4) holds true.

Proof: Let $\boldsymbol{x}^*$ denote an optimal solution for (5), and $\alpha^* = \text{argmax}_{\alpha \in \mathbf{A}}(CVaR_\alpha(f(\boldsymbol{x}^*, V)) - CVaR_\alpha(f(\boldsymbol{x}, V|\boldsymbol{x} = 0)))$. Since $CVaR_\alpha(f(\boldsymbol{x}^*, V)) - CVaR_\alpha(f(\boldsymbol{x}, V|\boldsymbol{x} = 0)) \le CVaR_{\alpha^*}(f(\boldsymbol{x}^*, V)) - CVaR_{\alpha^*}(f(\boldsymbol{x}, V|\boldsymbol{x} = 0)), \forall \alpha \in \mathbf{A}$ and $CVaR_{\alpha^*}(f(\boldsymbol{x}^*, V)) - CVaR_{\alpha^*}(f(\boldsymbol{x}, V|\boldsymbol{x} = 0)) \le 0$, it follows that $CVaR_\alpha(f(\boldsymbol{x}^*, V)) - CVaR_\alpha(f(\boldsymbol{x}, V|\boldsymbol{x} =$

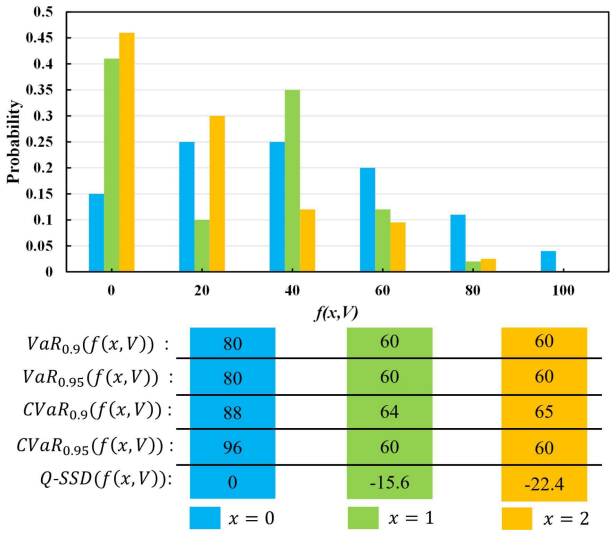

Fig. 2. Conditional loss probabilities and values of risk measures considered in Example 1.

$0)) \leq 0, \forall \alpha \in \mathbf{A}$. This implies $CVaR_\alpha(f(\boldsymbol{x}^*, V)) \leq CVaR_\alpha(f(\boldsymbol{x}, V|\boldsymbol{x}=0))$ and proves the statement. □

Proposition 2: A positive value for (5) indicates that at least one of the $|\mathbf{A}|$ constraints in (4) is violated.

Proof: Positive value of (5) for an optimal solution $\boldsymbol{x}^*$ means:

$$\max_{\alpha\in\mathbf{A}} \left(CVaR_\alpha(f(\boldsymbol{x}^*, V)) - CVaR_\alpha(f(\boldsymbol{x}, V|\boldsymbol{x}=0))\right) > 0.$$

Accordingly, there exists at least one $\alpha \in \mathbf{A}$ for which $CVaR_\alpha(f(\boldsymbol{x}^*, V)) - CVaR_\alpha(f(\boldsymbol{x}, V|\boldsymbol{x}=0)) > 0$ or equivalently, $CVaR_\alpha(f(\boldsymbol{x}^*, V)) > CVaR_\alpha(f(\boldsymbol{x}, V|\boldsymbol{x}=0))$. This violates (4) and proves the statement. □

Before explaining in Section II-C how the formulation (5) can be used to tackle the PPSD problem, we present here an example that clarifies the meaning of (5) and that shows its potential advantages over formulations which minimize CVaR or VaR in risk mitigation problems.

Example 1: Consider a problem in which $\boldsymbol{x} = (x)$ (i.e., there is one decision variable x) and only two decisions (see set $\mathcal{X} = \{1, 2\}$) can be taken in order to minimize the risk of a high loss. Assume that actions 1 and 2 are mutually exclusive.

Let $f(x, V|x=i)$ denote the conditional loss if $x = i, i = 0, 1, 2$ with $x = 0$ corresponding to the case when no action is taken and $x = 1$ (resp., 2) corresponding to the case when action 1 (resp., 2) is taken.

- When no action is taken, $f(x, V|x=0)$ can take values 0, 20, 40, 60, 80, and 100 with respective probabilities 0.15, 0.25, 0.25, 0.2, 0.11, and 0.04;
- When $x = 1$, $f(x, V|x=1)$ can take values 0, 20, 40, 60, and 80 with respective probabilities 0.41, 0.1, 0.35, 0.12, and 0.02;
- When $x = 2$, $f(x, V|x=2)$ can take values 0, 20, 40, 60, and 80 with respective probabilities 0.46, 0.3, 0.12, 0.095, and 0.025.

The above conditional loss distributions are displayed in Fig. 2. We show now the effect of actions 1 and 2 under different risk measures, namely VaR, CVaR, and Q-SSD. Suppose that the decision-maker is risk-averse and considers high confidence levels, such as 0.9 or 0.95, for the VaR and CVaR metrics. Using (2), we calculate the CVaR for the conditional loss $f(x, V|x=1)$ at the $\alpha = 0.9$ confidence level as follows:

$$\begin{aligned}
&CVaR_{0.9}(f(x, V|x=1))\\
&= \mathbb{E}\left[f(x, V|x=1) | f(x, V|x=1) \geq VaR_{0.9}(f(x, V|x=1))\right]\\
&= VaR_{0.9}(f(x, V|x=1))\\
&\quad + \frac{1}{1-0.9}\mathbb{E}[(f(x, V|x=1) - VaR_{0.9}(f(x, V|x=1)))^+]\\
&= 60 + 10 \times (0.41 \times (0-60)^+ + 0.1 \times (20-60)^+\\
&\quad + 0.35 \times (40-60)^+ + 0.12 \times (60-60)^+\\
&\quad + 0.02 \times (80-60)^+) = 64.
\end{aligned}$$

We obtain the $VaR_{0.9}$, $VaR_{0.95}$, $CVaR_{0.9}$, $CVaR_{0.95}$ associated with $f(x, V|x=0)$, $f(x, V|x=1)$, and $f(x, V|x=2)$ as shown at the top-four rows of the bottom table in Fig. 2 from left to right. On one hand, we have $VaR_{0.9}(f(x, V|x=1)) = VaR_{0.9}(f(x, V|x=2)) = 60$, $VaR_{0.95}(f(x, V|x=1)) = VaR_{0.95}(f(x, V|x=2)) = 60$, and $CVaR_{0.95}(f(x, V|x=1)) = CVaR_{0.95}(f(x, V|x=2)) = 60$ meaning that $VaR_{0.9}$, $VaR_{0.95}$, and $CVaR_{0.95}$ risk measures are indifferent between actions 1 and 2. On the other hand, $CVaR_{0.9}$ risk measure selects action 1, given $CVaR_{0.9}(f(x, V|x=1)) = 64 < CVaR_{0.9}(f(x, V|x=2)) = 65$.

Next, we calculate the value of Q-SSD using (6) and considering $\mathbf{A} = \{\frac{1}{20}, \frac{2}{20}, \ldots, \frac{19}{20}\}$. For the three cases $f(x, V|x=0)$, $f(x, V|x=1)$, and $f(x, V|x=2)$, we have:

$$\begin{aligned}
&\text{Q-SSD}(f(x, V|x=0))\\
&\quad = \max_{\alpha\in\mathbf{A}} (CVaR_\alpha(f(x, V|x=0)))\\
&\qquad - CVaR_\alpha(f(x, V|x=0))) = 0,\\
&\text{Q-SSD}(f(x, V|x=1)) = \max\{-15.8, -16.7, -17.6, -17.5,\\
&\qquad -17.3, -17.1, -16.9, -16.7, -16, -15.6, -16.9, -19,\\
&\qquad -21.7, -22, -22.4, -23, -24, -24, -36\} = -15.6,\\
&\text{Q-SSD}(f(x, V|x=2)) = \max\{-22.4, -23.7, -25.1, -25.4,\\
&\qquad -25.7, -26.1, -26.6, -27.2, -26, -26.2, -26.9, -27.8,\\
&\qquad -28.9, -27, -24.4, -24.5, -26, -23, -36\} = -22.4.
\end{aligned}$$

Clearly, the optimal solution based on the Q-SSD risk measure is to take action 2.

Two observations stand out in this example. First, actions 1 and 2 are both optimal for all considered metrics except for $CVaR_{0.9}$ (selecting only action 1) and Q-SSD (selecting only action 2). Second, based on the top plot in Fig. 2, the loss function associated with action 2 has a right-skewed loss distribution (i.e, the mass of the distribution is concentrated on smaller values of loss). While the probabilities of low loss values (i.e., 0 and 20) are significantly higher with action 2 than with action 1, one can

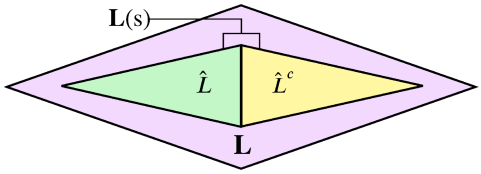

Fig. 3. Nested structure of the sets defined in the proposed PPSD formulation.

see that the probabilities of high loss values (i.e., 40, 60, and 100) are significantly lower with action 2 than with action 1. These observations highlight that the *Q-SSD*-based formulation (5) not only permits to differentiate the two solutions 1 and 2 (as opposed to most of the other metrics), but also defines a right-skewed probability distribution (i.e., probability masses concentrated on the small possible values) for the random loss function $f(\boldsymbol{x}, V)$ associated with the selected solution $\boldsymbol{x}$ (i.e., action 2). This implies that the model tends to select a solution that lowers $CVaR_\alpha(f(\boldsymbol{x}, V))$ for all $\alpha \in \mathbf{A}$.

C. Wildfire Risk Minimization

In this study, we consider uncertainty in the economic consequences of electrically-induced wildfires at different periods as wildfires may result in power outages of various magnitudes. The scenarios in the set $\mathbf{S}$ reflect the possible wind speeds and directions over time, the vulnerability of overhead power lines, and whether a power line is surrounded by dense vegetation (see Section IV-B). Let p_s be the probability of scenario $s \in \mathbf{S}$, i.e, $\sum_{s\in\mathbf{S}} p_s = 1$. For each scenario s, the cost of wildfires is defined by the economic loss resulting from arc ignitions on different overhead power lines.

Let $\mathbf{L}$ be the set of all overhand lines in the DS. We denote the subset of lines which ignite a fire under scenario s by $\mathbf{L}(s) \subseteq \mathbf{L}$ and the period of fault on line $l \in \mathbf{L}(s)$ under scenario s by $\tau(ls) \in \mathbf{T}$. Suppose one decides to select a subset of power lines $\hat{L} \subseteq \mathbf{L}(s)$ to be kept energized at their fault periods in scenario s (i.e., $x_{l\tau(ls)} = 0$ for all $l \in \hat{L}$), and de-energize the lines in the complementary subset $\hat{L}^c = \mathbf{L}(s)\backslash\hat{L}$ at their fault periods in scenario s (i.e., $x_{l\tau(ls)} = 1$ for all $l \in \hat{L}^c$). In the PPSD problem, we assume that the decision-maker has an estimate of the wildfire cost under scenario s given any subset $\hat{L}$ (i.e., the only energized lines in $\mathbf{L}(s)$), and we denote it by $C^F_{\hat{L}s}$. Fig. 3 illustrates the relationship between the sets mentioned above.

Now, given the PSPS actions (x_{lt} for all $l \in \mathbf{L}$ and $t \in \mathbf{T}$), we find the selected subset $\hat{L}$ for each scenario s using:

$$\pi_{\hat{L}s} = \prod_{l\in\hat{L}}(1 - x_{l\tau(ls)}) \prod_{l\in\hat{L}^c} x_{l\tau(ls)}. \tag{7}$$

and the wildfire cost under this scenario as:

$$C^F_s = \sum_{\hat{L}\subseteq\mathbf{L}(s)} C^F_{\hat{L}s}\pi_{\hat{L}s}. \tag{8}$$

To provide a better understanding of (8), we illustrate how to calculate the value of C^F_s using this equation in Appendix A. For any scenario s and the subset of power lines $\hat{L} \subseteq \mathbf{L}(s)$, the polynomial term defined in the right-hand-side of (7) can take value 0 or 1. If, for every line $l \in \hat{L}$, the corresponding term $(1 - x_{l\tau(ls)})$ is equal to 1 (i.e., $x_{l\tau(ls)} = 0$), wildfire ignitions occur at *every* line $l \in \hat{L}$ at period $\tau(ls)$. Similarly, if for every line $l \in \hat{L}^c$, the term $x_{l\tau(sl)}$ is equal to 1, there is no ignition at any line $l \in \hat{L}^c$. We show in Proposition 3 that the two polynomial terms can both be equal to 1 for only one set $\hat{L} \subseteq \mathbf{L}(s)$. When this occurs, we have $\hat{L} \subseteq \mathbf{L}(s)$.

Proposition 3: For any $s \in \mathbf{S}$, the equality

$$\prod_{l\in\hat{L}}(1 - x_{l\tau(ls)}) \prod_{l\in\hat{L}^c} x_{l\tau(ls)} = 1 \tag{9}$$

holds true for one and only one subset $\hat{L} \subseteq \mathbf{L}(s)$.

Proof: Consider an arbitrary feasible solution $\tilde{x}_{lt}, l \in \mathbf{L}, t \in \mathbf{T}$ for the PPSD problem. Define the index set $W = \{(l, t) : \tilde{x}_{lt} = 1, l \in \mathbf{L}, t \in \mathbf{T}\}$. For any $s \in \mathbf{S}$ and $\hat{L} \subseteq \mathbf{L}(s)$, (9) holds if $(l, \tau(ls)) \notin W, \forall l \in \hat{L}$ and $(l', \tau(l's)) \in W, \forall l' \in \hat{L}^c$.

First, we show – by contradiction – that for each feasible solution of problem PPSD and each $s \in \mathbf{S}$, the conditions mentioned above hold for *at most one* subset $\hat{L} \subseteq \mathbf{L}(s)$. Suppose that there exists another set $\hat{L}_0 \subseteq \mathbf{L}(s)$ and $\hat{L} \neq \hat{L}_0$ for $s \in \mathbf{S}$, such that we have: $(l, \tau(ls)) \notin W,\ \forall l \in \hat{L}_0$ and $(l', \tau(l's)) \in W,\ \forall l' \in \hat{L}^c_0$. This means that (9) holds for both $\hat{L}, \hat{L}_0 \subseteq \mathbf{L}(s)$. There are three possible cases for the relation between $\hat{L}$ and $\hat{L}_0$:

(1) $\hat{L} \subset \hat{L}_0$: There exists $l \in \hat{L}^c$ while $l \in \hat{L}_0$ (i.e., $(l, \tau(ls)) \notin W, x_{l\tau(ls)} = 0$), which implies $\prod_{l\in\hat{L}^c} x_{l\tau(ls)} = 0$.

(2) $\hat{L}_0 \subset \hat{L}$. There exists $l \in \hat{L}^c_0$ while $l \in \hat{L}$ (i.e., $(l, \tau(ls)) \in W, x_{l\tau(ls)} = 1$), which implies $\prod_{l\in\hat{L}}(1 - x_{l\tau(ls)}) = 0$.

(3) neither $\hat{L} \subset \hat{L}_0$ nor $\hat{L}_0 \subset \hat{L}$: There exists a line $l \in \hat{L}$ (i.e., $(l, \tau(ls)) \in W, x_{l\tau(ls)} = 1$) while $l \notin \hat{L}_0$, which implies $\prod_{l\in\hat{L}}(1 - x_{l\tau(ls)}) = 0$.

We have proven in each of the three cases the invalidity of the initial assumption according to which (9) holds if $\hat{L}_0 \neq \hat{L}$.

What is left to prove is that such a set $\hat{L}$ *always exists* for each $s \in \mathbf{S}$. Two cases can occur for each $s \in \mathbf{S}$:

1) $(l, \tau(ls)) \in W,\ \forall l \in \mathbf{L}(s)$: we have $\hat{L} = \emptyset$. Since $\emptyset \subseteq \hat{L}$, the set $\hat{L}$ exists.
2) $\exists l \in \mathbf{L}(s)$, such that $(l, \tau(ls)) \notin W$: there is a set $\hat{L}$ that includes every $l \in \mathbf{L}(s)$ and such that $(l, \tau(ls)) \notin W$. This means that the set $\hat{L}$ exists in this case as well. □

Using the definition (8) of the wildfire cost under a certain scenario s, we rewrite the two following CVaRs as:

$$CVaR_\alpha(f(\boldsymbol{x}, V)) = \min_{\eta\in\mathbb{R}_+} \eta + \frac{1}{1-\alpha}\sum_{s\in\mathbf{S}} p_s \left(C^F_s - \eta\right)^+ \tag{10}$$

$$CVaR_\alpha(f(\boldsymbol{x}, V|\boldsymbol{x} = 0)) = \min_{\hat{\eta}\in\mathbb{R}_+} \hat{\eta} + \frac{1}{1-\alpha}\sum_{s\in\mathbf{S}} p_s \left(\hat{C}^F_s - \hat{\eta}\right)^+ \tag{11}$$

where $\hat{C}^F_s$ denotes the cost of wildfires without taking any PSPS action and is calculated by fixing $x_{l,t} = 0, l \in \mathbf{L}, t \in \mathbf{T}$ in (7). We can calculate ex-ante the value of $CVaR_\alpha(\hat{f}(V))$ for every $\alpha \in \mathbf{A}$ which becomes a known parameter in the optimization model. The next step is to rewrite the bi-level min-max problem

(5) as:

$$\min \mathcal{W} \tag{12}$$

with $\mathcal{W}$

$$= \max_{\alpha \in \mathbf{A}} \left(CVaR_\alpha(f(\boldsymbol{x}, V)) - CVaR_\alpha(f(\boldsymbol{x}, V|\boldsymbol{x}=0)) \right). \tag{13}$$

D. PSPS-Caused Power Outage Cost Minimization

De-energizing power lines through PSPS actions leads to electricity outages across the DS. The proposed PPSD aims at balancing the risk of wildfires and the undesirable consequences of the associated power outages. To alleviate the PSPS-caused power outages, we consider MPSs as a backup source of energy and we account for their operating cost in the formulation of the cost function for PSPS-caused power outages. The expected total cost of PSPS actions is then

$$\mathcal{O} = \sum_{t\in\mathbf{T}} \sum_{i\in\mathbf{I}} \left((\beta_t + \gamma_i) D^p_{it} y^\Gamma_{it} + \sum_{m\in\mathbf{M}^g} \delta^g_m \varphi^\Gamma_{imt} + \sum_{m\in\mathbf{M}^e} \delta^e_m (\rho^c_{imt} + \rho^d_{imt}) \right) \tag{14}$$

where the first term is the cost of power outages including the loss of revenue for the electric utility ($\beta_t D^p_{it} y^\Gamma_{it}$) and the interruption cost for customers ($\gamma_i D^p_{it} y^\Gamma_{it}$). The decision variable $y^\Gamma_{it} \in [0,1]$ defines the partial outage in real power demand D^Γ_{it} in node i at period t. The second term reflects the generation cost associated with the output power of MEGs ($\sum_{m\in\mathbf{M}^g} \delta^g_m \varphi^\Gamma_{imt}$). The third term is the cost related to battery degradation due to the MESS charge and discharge actions.

III. Mathematical Model and Reformulation Method

In this section, we first present in detail the proposed S-MINLP formulation (15) for the PPSD problem before deriving an MILP reformulation.

A. Model Formulation

We propose a Q-SSD-based risk-averse optimization model PPSD to hedge against the uncertain consequences of wildfires driven by various weather conditions. To ease the notations, we introduce $\varrho \in \{\Gamma, \Lambda\}$ with Γ and Λ referring to real and reactive power, respectively. The PPSD problem is formulated as an S-MINLP problem:

$$\min \mathcal{O} + \mathcal{W} \tag{15a}$$

s.t. (7), (8), (10), (13), (14)

$$\sum_{l\in\mathbf{L};i(l)=i} f^\varrho_{lt} + D^\varrho_{it}(1-y^\varrho_{it}) = \sum_{l\in\mathbf{L};j(l)=i} f^\varrho_{lt} + \phi^\varrho_{it} \quad \forall i\in\mathbf{I}, t\in\mathbf{T}, \varrho\in\{\Gamma,\Lambda\} \tag{15b}$$

$$-(1-x_{lt})F^\varrho_l \le f^\varrho_{lt} \le (1-x_{lt})F^\varrho_l \quad \forall l\in\mathbf{L}, t\in\mathbf{T}, \varrho\in\{\Gamma,\Lambda\} \tag{15c}$$

$$v_{i(l)t} - v_{j(l)t} \ge -x_{lt}M^v + 2(R_l f^\Gamma_{lt} + X_l f^\Lambda_{lt}) \quad \forall l\in\mathbf{L}, t\in\mathbf{T} \tag{15d}$$

$$v_{i(l)t} - v_{j(l)t} \le x_{lt}M^v + 2(R_l f^\Gamma_{lt} + X_l f^\Lambda_{lt}) \quad \forall l\in\mathbf{L}, t\in\mathbf{T} \tag{15e}$$

$$\phi^\varrho_{it} = \sum_{n\in\mathbf{N}_i} G^\varrho_{nt} + \psi^\varrho_{it} \quad \forall i\in\mathbf{I}, t\in\mathbf{T}, \varrho\in\{\Gamma,\Lambda\} \tag{15f}$$

$$\mu_{jm(t+\tau)} \le 1 - \mu_{imt} \quad \forall i,j\in\mathbf{I}^m, m\in\mathbf{M}, \tau \le T^m_{ij}, t \le |\mathbf{T}| - \tau \tag{15g}$$

$$\sum_{i\in\mathbf{I}^m} \mu_{imt} \le 1 \quad \forall m\in\mathbf{M}, t\in\mathbf{T} \tag{15h}$$

$$\sum_{m\in\mathbf{M}} \mu_{imt} \le c_i \quad \forall i\in\mathbf{I}, t\in\mathbf{T} \tag{15i}$$

$$\psi^\varrho_{it} = \sum_{m\in\mathbf{M}^g; i\in\mathbf{I}^m} \varphi^\varrho_{imt} + \sum_{m\in\mathbf{M}^e; i\in\mathbf{I}^m} \omega^\varrho_{imt} \quad \forall i\in\mathbf{I}, t\in\mathbf{T}, \varrho\in\{\Gamma,\Lambda\} \tag{15j}$$

$$\underline{A^\varrho_m}\mu_{imt} \le \varphi^\varrho_{imt} \le \overline{A^\varrho_m}\mu_{imt} \quad \forall i\in\mathbf{I}^m, m\in\mathbf{M}^g, t\in\mathbf{T}, \varrho\in\{\Gamma,\Lambda\} \tag{15k}$$

$$Z_{m(t+1)} - Z_{mt} = \sum_{i\in\mathbf{I}^m} \left(\varepsilon^c_m \rho^c_{imt} - \rho^d_{imt}/\varepsilon^d_m \right) \quad \forall m\in\mathbf{M}^e, t\in\mathbf{T}\backslash\{|\mathbf{T}|\} \tag{15l}$$

$$\kappa^c_{imt} + \kappa^d_{imt} \le \mu_{imt} \quad \forall (i,m,t)\in\mathbb{V} \tag{15m}$$

$$\underline{J^c_m}\kappa^c_{imt} \le \rho^c_{imt} \le \overline{J^c_m}\kappa^c_{imt} \quad \forall (i,m,t)\in\mathbb{V} \tag{15n}$$

$$\underline{J^d_m}\kappa^d_{imt} \le \rho^d_{imt} \le \overline{J^d_m}\kappa^d_{imt} \quad \forall (i,m,t)\in\mathbb{V} \tag{15o}$$

$$\omega^\Gamma_{imt} = \rho^d_{imt} - \rho^c_{imt} \quad \forall (i,m,t)\in\mathbb{V} \tag{15p}$$

$$\underline{W^\Lambda_m}\mu_{imt} \le \omega^\Lambda_{imt} \le \overline{W^\Lambda_m}\mu_{imt} \quad \forall (i,m,t)\in\mathbb{V} \tag{15q}$$

$$\mu_{imt} = 0 \quad \forall i\in\mathbf{I}\backslash\mathbf{I}^m, m\in\mathbf{M}, t\in\mathbf{T} \tag{15r}$$

$$\mu_{im1} = 1 \quad \forall i\in\mathbf{I}', m\in\mathbf{M} \tag{15s}$$

$$\underline{Z_m} \le Z_{mt} \le \overline{Z_m} \quad \forall m\in\mathbf{M}, t\in\mathbf{T} \tag{15t}$$

$$\underline{v_i} \le v_{it} \le \overline{v_i} \quad \forall i\in\mathbf{I}, t\in\mathbf{T} \tag{15u}$$

$$\underline{G^\varrho_n} \le G^\varrho_{nt} \le \overline{G^\varrho_n} \quad \forall n\in\mathbf{N}, t\in\mathbf{T}\varrho\in\{\Gamma,\Lambda\} \tag{15v}$$

$$x_{lt}, \kappa^c_{imt}, \kappa^d_{imt}, \mu_{imt} \in \{0,1\} \tag{15w}$$

$$f^\varrho_{lt}, \phi^\varrho_{it}, \psi^\varrho_{it}, \omega^\varrho_{it} \in \mathbb{R}; G^\varrho_{nt}, \varphi^\varrho_{imt} \in \mathbb{R}_+; y^\varrho_{it} \in [0,1] \quad \forall \varrho\in\{\Gamma,\Lambda\} \tag{15x}$$

$$v_{it}, Z_{mt}, \rho^c_{imt}, \rho^d_{imt} \in \mathbb{R}_+ \tag{15y}$$

The objective function minimizes the sum of the costs due to wildfires $\mathcal{W}$ defined by (7), (8), (10), (13) and the *PSPS-caused power outage costs* $\mathcal{O}$ defined by (14), wherein, the ex-ante known values of $CVaR_\alpha(f(\boldsymbol{x}, V|\boldsymbol{x}=0))$ for every $\alpha \in \mathbf{A}$ are obtained through fixing $x_{l,t} = 0, \forall l \in \mathbf{L}, t \in \mathbf{T}$ based on (11).

Several properties of the objective function are presented in Appendix B. Constraint (15b) describes the real and reactive power balance conditions at each node in the DS, stipulating that the total incoming and outgoing power flows must be equal. The notations $i(l)$ and $j(l)$ represent the source and terminal nodes of overhead power line l, respectively. The real and reactive power flows in overhead power lines are bounded by their real and reactive power capacities in (15c). Constraints (15d) and (15e) represent the power flow equation considering the status of the overhead power lines based on the DistFlow model [39]. The real and reactive power generation at each node consist of the generated power from the substation and the energy supply by MPSs, which is denoted by constraint (15f). The set of constraints (15g) defines the dispatch scheduling of MPSs. In a DS, candidate nodes are nodes equipped with specific electrical facilities that allow MPSs to be connected to the DS. For example, if MPS m is at candidate node i at time $t = 1$ (i.e., $\mu_{im1} = 1$) and needs 2 time periods to travel from candidate node i to node j (i.e., $T^m_{ij} = 2$)—meaning that MPS m is on its way from nodes i to j at $t = 2$ and $t = 3$, then MPS m will arrive at candidate node j at $t = 4$ (i.e., $\mu_{jm4} = 1$), which implies $\mu_{jm1} = 0$, $\mu_{jm2} = 0$, and $\mu_{jm3} = 0$. Constraint (15h) enforces that each MPS m can stay in at most one node at any period. Constraint (15i) ensures that the total number of MPSs located at candidate node i at any period does not exceed the maximum number of vehicles that node i can host. Constraint (15j) reflects that the real and reactive power injections from MPS m to candidate node i involve real and reactive power supplied by MEGs and MESSs. Constraint (15k) determines the range of real and reactive output power of MEGs. Constraint (15l) represents the variations in the state of charge of MESS m over time, which are determined by MESSs' charging and discharging behaviors. To ease the notations, we define the index set $\mathbb{V} = \{(i, m, t) : i \in \mathbf{I}^m, m \in \mathbf{M}^e, t \in \mathbf{T}\}$. Constraint (15m) ensures that MESS m can neither charge nor discharge at candidate node i if it is not connected ($\mu_{imt} = 0$) to the node, and expresses that the charging and discharging states are mutually exclusive: any MESS m connected to candidate node i cannot be in charging and discharging state at the same time. Constraints (15n) and (15o) restrict the range of the MESSs' charging and discharging power, respectively. The real power output of MESSs is bounded by constraint (15p). Constraint (15q) specifies the bound on the reactive power output of MPSs. Constraint (15r) ensures that an MPS cannot be dispatched to a non-candidate node in the DS while constraint (15s) defines the initial positioning of each MPS. The notation $\mathbf{I}'$ denotes the set of nodes where MPSs can be initially pre-positioned. Constraints (15t)–(15v) represents the limits on the state of charge of the MESS m at time t (Z_{mt}), the squared voltage magnitudes of node i at time t (v_{it}), and the generation of real (G^{Γ}_{nt}) and reactive power (G^{Λ}_{nt}) in the substation. The nonlinearities in model (15) are due to the polynomial terms in the equality constraints (8), to the max operand term $(C^F_s - \eta^F)^+ = \max\{C^F_s - \eta^F, 0\})$ in constraint (10), and to the inner maximization in constraint (13).

Lemma 4: The continuous relaxation of the S-MINLP model (15) is nonconvex.

Proof: Model (15) includes several nonlinear equality constraints (7), (10), and (13), and has thus a nonconvex feasible area regardless of the binary restrictions on some variables. □

B. Reformulation

We now derive an MILP reformulation equivalent to problem (15). Proposition 5 shows how to linearize the nonlinear terms in the S-MINLP model by exploiting its structure.

Proposition 5: Let $\xi^F_s \in \mathbb{R}_+$ and $\pi_{\hat{L}s} \in \{0, 1\}$ be the auxiliary decision variables. The MILP reformulation problem

$$\min \mathcal{O} + \mathcal{W}$$

$$\text{s.t. } (8),\ (14),\ (15b)-(15y)$$

$$\xi^F_s \geq C^F_s - \eta \qquad \forall s \in \mathbf{S} \quad (16a)$$

$$\pi_{\hat{L}s} \geq -|\mathbf{L}(s)| + 1 + \sum_{l\in\hat{L}}(1 - x_{l\tau(ls)}) + \sum_{l\in\hat{L}^c} x_{l\tau(ls)} \qquad \forall \hat{L} \subseteq \mathbf{L}(s),\ s \in \mathbf{S} \quad (16b)$$

$$\mathcal{W} \geq \eta + \frac{1}{1-\alpha}\sum_{s\in\mathbf{S}} p_s \xi^F_s - CVaR_\alpha(\hat{f}(V)) \quad \forall \alpha \in \mathbf{A} \quad (16c)$$

$$\xi^F_s \in \mathbb{R}_+, s \in \mathbf{S},\ \pi_{\hat{L}s} \in \{0, 1\}\ \forall \hat{L} \subseteq \mathbf{L}(s), s \in \mathbf{S} \quad (16d)$$

is equivalent to (15).

Proof: (i): We first reformulate the nonlinear constraint (7). This relationship can be enforced via (16b).

It is immediate to see that:

$$\prod_{l\in\hat{L}}(1 - x_{l\tau(ls)}) \prod_{l\in\hat{L}^c} x_{l\tau(ls)} = 1 \quad (17)$$

$$\Leftrightarrow\ x_{l\tau(ls)} = 0,\ \forall l \in \hat{L} \text{ and } x_{l\tau(ls)} = 1,\ \forall l \in \hat{L}^c$$

$$\Leftrightarrow\ \sum_{l\in\hat{L}}(1 - x_{l\tau(ls)}) = |\hat{L}| \text{ and } \sum_{l\in\hat{L}^c} x_{l\tau(ls)} = |\hat{L}^c|$$

$$\Leftrightarrow\ -|\mathbf{L}(s)| + 1 + \sum_{l\in\hat{L}}(1 - x_{l\tau(ls)}) + \sum_{l\in\hat{L}^c} x_{l\tau(ls)} = 1 \quad (18)$$

with the validity of the last relationship due to $|\hat{L}| + |\hat{L}^c| = |\mathbf{L}(s)|$. Therefore, if (18) holds, then $\pi_{\hat{L}s}$ must take value 1.

On the other hand, if $\prod_{l\in\hat{L}}(1 - x_{l\tau(ls)}) \prod_{l\in\hat{L}^c} x_{l\tau(ls)} = 0$, we show that $\pi_{\hat{L}s}$ can take value 0 or 1.

Next, we show that it is possible for $\pi_{\hat{L}s}$ to take 0 for some $s \in \mathbf{S}$ and $\hat{L} \subseteq \mathbf{L}(s)$. From Proposition 3, we know that for any $s \in \mathbf{S}$, the equality

$$\prod_{l\in\hat{L}}(1 - x_{l\tau(ls)}) \prod_{l\in\hat{L}^c} x_{l\tau(ls)} = 1$$

holds true for one and only one subset $\hat{L} \subseteq \mathbf{L}(s)$. This means that for any $s \in \mathbf{S}$, the expression $\prod_{l\in\hat{L}}(1 - x_{l\tau(ls)}) \prod_{l\in\hat{L}^c} x_{l\tau(ls)}$ is equal to 0 for all $\hat{L} \subseteq \mathbf{L}(s)$, except for one. Then, we have:

$$\prod_{l\in\hat{L}}(1 - x_{l\tau(ls)}) \prod_{l\in\hat{L}^c} x_{l\tau(ls)} = 0$$

$$\Leftrightarrow \quad x_{l\tau(ls)} = 1, \exists l \in \hat{L}, \text{ or } x_{l\tau(ls)} = 0, \exists l \in \hat{L}^c$$

$$\Leftrightarrow \quad \sum_{l\in\hat{L}}(1 - x_{l\tau(ls)}) < |\hat{L}|, \text{ or } \sum_{l\in\hat{L}^c} x_{l\tau(ls)} < |\hat{L}^c|$$

$$\Leftrightarrow \quad -|\mathbf{L}(s)| + 1 + \sum_{l\in\hat{L}}(1 - x_{l\tau(ls)}) + \sum_{l\in\hat{L}^c} x_{l\tau(ls)} \leq 0$$

with the validity of the last relationship due to always having $\sum_{l\in\hat{L}}(1 - x_{l\tau(ls)}) \leq |\hat{L}|$ and $\sum_{l\in\hat{L}^c} x_{l\tau(ls)} \leq |\hat{L}^c|$. This proves that it is possible for $\pi_{\hat{L}s}$ to take 0 as long as we have $\prod_{l\in\hat{L}}(1 - x_{l\tau(ls)}) \prod_{l\in\hat{L}^c} x_{l\tau(ls)} = 0$.

In the optimal solution, if free to take value 0 or 1, $\pi_{\hat{L}s}$ will take value 0 since the objective value (to be minimized) is an increasing function of the overall wildfire costs C_s^F which is itself monotone increasing with $\pi_{\hat{L}s}$. This shows that constraint (16b) along with the binary restriction on $\pi_{\hat{L}s}$ provide an exact linearization of the nonlinear constraint (8).

(ii): To reformulate each term $(C_s^F - \eta^F)^+$ for any $s \in \mathbf{S}$ in (10), we introduce a nonnegative auxiliary decision variable $\xi_s^F \in \mathbb{R}_+$, substitute ξ_s^F for $(C_s^F - \eta^F)^+$, and add constraint (16a), which allows rewriting (10) as

$$CVaR_\alpha\left(f(\boldsymbol{x}, V)\right) = \min_{\eta\in\mathbb{R}_+} \eta + \frac{1}{1-\alpha}\sum_{s\in\mathbf{S}} p_s \xi_s^F. \tag{19}$$

and (13) as

$$\mathcal{W} = \max_{\alpha\in\mathbf{A}} \left(\min_{\eta\in\mathbb{R}_+} \left(\eta + \frac{1}{1-\alpha}\sum_{s\in\mathbf{S}} p_s \xi_s^F \right) - CVaR_\alpha\left(f\left(\boldsymbol{x}, V|\boldsymbol{x}=0\right)\right)\right) \tag{20}$$

(iii) Lastly, we linearize (20). Using the epigraphic approach, we replace (20) with the inequalities

$$\mathcal{W} \geq \min_{\eta\in\mathbb{R}_+} \left(\eta + \frac{1}{1-\alpha}\sum_{s\in\mathbf{S}} p_s \xi_s^F \right) - CVaR_\alpha\left(f\left(\boldsymbol{x}, V|\boldsymbol{x}=0\right)\right) \quad \forall \alpha \in \mathbf{A} \tag{21}$$

which is equivalent to (16c) due to the sign on the inequality and the minimization term on the right side of (20).

The objective function and all the constraints are now linear, which provides the result that we set out to prove. □

IV. Numerical Results and Discussions

A. Test System Characteristics and Assumptions

In this section, we test the proposed model (16) on the IEEE 33-node test system (see Fig. 4), which consists of 33 nodes, 32 overhead power lines, and 1 substation. The detailed information on each node and line in the system is provided in [39]. As shown in Fig. 4, the system has six critical load nodes and ten candidate nodes to which an MPS can be connected for charging and power delivery (discharging). Node 1 is an MPS depot owning two MEGs (i.e., M1 and M2) with 800 kW/600 kVar capacity and one MESS (i.e., M3) with 500 kW/1000 kWh capacity. Algorithm 1 (see next Section IV-B) returns 760 unique

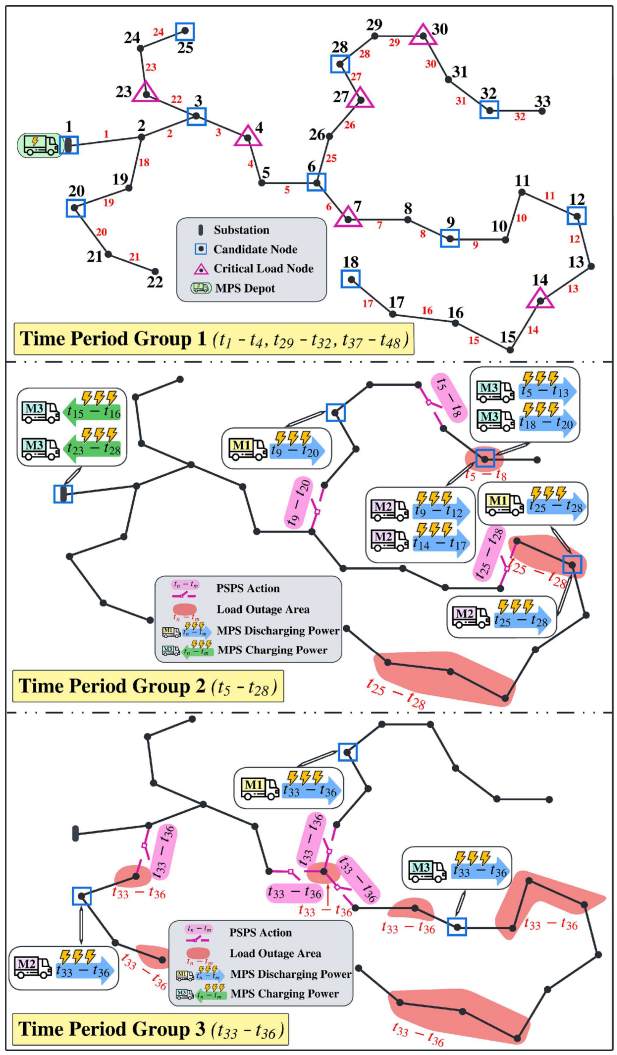

Fig. 4. Optimal decisions on PSPS action and MPS dispatch in the wind-exposed wildfire-prone IEEE 33-node test system.

representative wildfire scenarios ($|\mathbf{S}| = 760$), and related parameters (i.e., p_s, $\tau(ls)$). Inspired by the existing practice [8], the PSPS decisions are made 12 hours ahead by solving the PPSD problem in which the planning horizon includes 48 15-minute periods. The optimization problem (16) is coded with the AMPL algebraic modeling language and solved with the optimization solver Gurobi 9.0.2.

B. Wildfire Scenarios

An electrically-induced wildfire is consecutive to the combination of two independent events: a fault on an overhead power line and subsequent arc-ignition of nearby vegetation around the power line. Let $q_{l,t}^{\text{Fau}}$ and $q_{l,t}^{\text{Ign}}$ respectively denote the probability of line fault and arc-ignition for every $l \in \mathbf{L}$ and $t \in \mathbf{T}$. We implement the model presented in [6], [40] to find $q_{l,t}^{\text{Fau}}$ and $q_{l,t}^{\text{Ign}}$ for every $l \in \mathbf{L}$ and $t \in \mathbf{T}$ in our experiments using weather information (e.g., wind speed, ambient temperature, relative humidity, etc.) captured in the vicinity of Paradise, California [41]. Given the likelihood of fault and arc-ignition for

Algorithm 1: Generation of Representative Scenario Set $\mathbf{S}$.

Initialize $s = 1$, $p_s = 1$, $\mathbf{L}(s) = \emptyset$, $\Theta_{lst} = 1,\ \forall l \in \mathbf{L},\ t \in \mathbf{T}, B(s) = \emptyset$.
for all $t \in \mathbf{T},\ l \in \mathbf{L}$ **do**
  $\hat{s} \leftarrow s$
  for all $s' \in \{1, \ldots, \hat{s}\}$ **do**
    if $l \notin B(s')$ **then**
      if $q^{\text{Fau}}_{l,t} > \epsilon$ **then**
        Find set $\tilde{L}(l)$ including line l's outgoing branches
        Set $s \leftarrow s+1$, $p_s \leftarrow p_{s'} \times q^{\text{Fau}}_{l,t} \times q^{\text{Ign}}_{l,t}$, $\Theta_{lst} \leftarrow 0$, $\mathbf{L}(s) \leftarrow \mathbf{L}(s') \cup \{l\}$, $B(s) \leftarrow B(s') \cup \tilde{L}(l)$
        Set $s \leftarrow s+1$, $p_s \leftarrow p_{s'} \times q^{\text{Fau}}_{l,t} \times (1 - q^{\text{Ign}}_{l,t})$, $\Theta_{lst} \leftarrow 0$, $\mathbf{L}(s) \leftarrow \mathbf{L}(s')$, $B(s) \leftarrow B(s') \cup \tilde{L}(l)$
        Set $p_{s'} \leftarrow p_{s'} \times (1 - q^{\text{Fau}}_{l,t})$
      end if
    end if
  end for
end for
Initialize $\mathbf{S} = \emptyset$
for all $s' \in \{1, \ldots, s\}$ **do**
  if $\nexists s'' \in \mathbf{S} : \mathbf{L}(s') = \mathbf{L}(s''), \Theta_{ls't} = \Theta_{ls''t}, l \in \mathbf{L}(s'), t \in \mathbf{T}$ **then**
    Set $\mathbf{S} = \mathbf{S} \cup \{s'\}$
  end if
end for
for all $s' \in \mathbf{S}$ **do**
  $\hat{p}_{s'} \leftarrow 0$
  for all $s'' \in \{1, \ldots, s\}$ **do**
    if $\mathbf{L}(s') = \mathbf{L}(s'')$ and $\Theta_{ls't} = \Theta_{ls''t},\ l \in \mathbf{L}(s'), t \in \mathbf{T}$ **then**
      $\hat{p}_{s'} \leftarrow \hat{p}_{s'} + p_{s''}$
    end if
  end for
  Set $p_{s'} \leftarrow \hat{p}_{s'}$
  $\tau(ls) \leftarrow \min\{t \in \mathbf{T} : \Theta_{lst} = 0\}$ for all $l \in \mathbf{L}(s)$
end for

every $l \in \mathbf{L}$ and $t \in \mathbf{T}$, we aim to generate a set $\mathbf{S}$ of plausible wildfire scenarios and derive the probability p_s, expressed as the product of probabilities $q^{\text{Fau}}_{l,t}$ and $q^{\text{Ign}}_{l,t}$. We provide below the pseudo-code of Algorithm 1 which is used to generate the scenario set $\mathbf{S}$, and we explain next its modalities. The notation Θ_{lst} refers to a binary indicator for the status of overhead power line l at time t in scenario s, and takes value 0 if there is a fault and 1 otherwise. Additionally, we define a set $B(s)$ for each scenario s representing the set of lines that do not ignite a fire in this scenario. The detailed pseudo-code of Algorithm 1 is provided in Appendix C.

C. Joint PSPS & MPS Dispatch Decisions

We first evaluate the efficiency of our proposed model in reducing the expected cost of wildfires (i.e., $\sum_{s\in\mathbf{S}} p_s C^F_s$). With joint decisions on PSPS actions and MPS dispatch, the expected cost of wildfire decreases from \$11,466,492 (original DS with no PSPS in action) to \$2,473,985 (using the proposed Q-SSD model), i.e., a cost reduction of 78%. Meanwhile, the extent of PSPS-caused power outages is found 4,299.16 kW when employing MPSs, accounting for nearly 2.8% of the total electrical demand during the 12-hour planning horizon. This corresponds to a 73% reduction in PSPS-caused electricity outages when using the proposed Q-SSD model compared to the case where no MPS is employed. We next present the optimal PSPS actions and MPS allocations resulting from the proposed Q-SSD model by separating the entire 48 time periods into 3 time period groups (TPG): **TPG1** ($t_1 - t_4, t_{29} - t_{32}, t_{37} - t_{48}$), **TPG2** ($t_5 - t_{28}$), and **TPG3** ($t_{33} - t_{36}$). Fig. 4 illustrates the optimal decisions during all temporal groups.

- **TPG1:** During these time periods, neither PSPS actions nor MPS allocations are implemented.
- **TPG2:** The overhead power lines 10 (PSPS1), 25 (PSPS2), and 30 (PSPS3) are shut-off at periods $t_{25} - t_{28}$, $t_9 - t_{20}$, and $t_5 - t_8$, respectively. With these PSPS actions implemented, several DS nodes are disconnected from the main substation and are therefore in outage for some time periods. In order to mitigate the PSPS-caused power outages, the MPSs are allocated to candidate nodes at different islands to deliver backup power. The nodal power demand would vary with time, which also affects the MPSs allocation. MPS M1 is sent to Node 28 to supply power during periods t_9 to t_{20}, and is then moved to Node 12 to discharge power from t_{25} to t_{28}. During periods $t_9 - t_{12}$ and $t_{14} - t_{17}$, M2 resides at Node 32 to provide power to the isolated area. Later, M2 is assigned to get connected to Node 12 from periods t_{25} to t_{28}. The MESS M3 is required to charge from the system when it runs out of stored energy. M3 is first sent to Node 32 to discharge power from t_5 to t_{13}, and then goes back to the depot (i.e., Node 1) to get charged during t_{15} to t_{16}. Next, it is allocated to Node 32 again from t_{18} to t_{20}. Eventually, M3 re-charges from t_{23} to t_{28}. The results indicate that the energy supplied by MPSs would serve first the critical load nodes. During periods t_5 to t_8 (PSPS3 in action), the residential area at Node 32 and from periods t_{25} to t_{28} (PSPS1 in action), communities connected to Nodes 11, 12, 15, 16, and 17 would experience a power outage.
- **TPG3:** Overhead power lines 5, 6, 18, and 25 are shut-off (PSPS4) from t_{33} to t_{36}, during which M1, M2, and M3 are assigned to Nodes 28, 20, and 9 for power delivery, while some non-critical load nodes will remain in outage.

D. Sensitivity Analysis and Benchmark Comparison

We here compare the solution of the problem PPSD using the proposed Q-SSD-based model with that of several benchmark measures (i.e., expected value, VaR, and CVaR) which are commonly used in decision-making under uncertainty:

- The first benchmark solution is the one obtained by including the expected cost of wildfire and is given by:

$$\min \quad \mathcal{O} + E[f(x,V)] = \mathcal{O} + \sum_{s\in\mathbf{S}} p_s C^F_s. \tag{22}$$

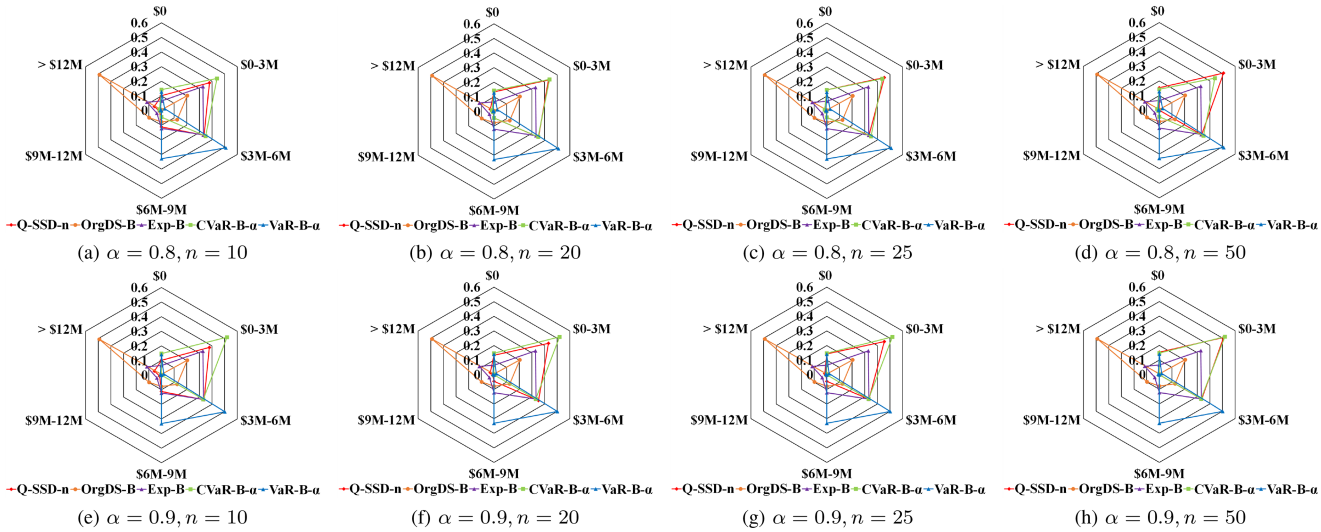

(a) $\alpha = 0.8, n = 10$ (b) $\alpha = 0.8, n = 20$ (c) $\alpha = 0.8, n = 25$ (d) $\alpha = 0.8, n = 50$

(e) $\alpha = 0.9, n = 10$ (f) $\alpha = 0.9, n = 20$ (g) $\alpha = 0.9, n = 25$ (h) $\alpha = 0.9, n = 50$

Fig. 5. Probability distribution of the wildfire cost using different risk measure benchmarks.

We refer to the benchmark problem (22) as Exp-B.

- The second benchmark solution is obtained by (23) in which the wildfire cost is measured by VaR:

$$\min \quad (\mathcal{O} + VaR_\alpha(f(x, V))) . \tag{23}$$

We evaluate the benchmark solution given different values of the confidence level $\alpha = 0.8$ and 0.9. For a given α, we refer to this benchmark as VaR-B-α.

- The third benchmark solution is obtained by (24) in which the wildfire cost is measured by CVaR [36]:

$$\min \quad (\mathcal{O} + CVaR_\alpha(f(x, V))) . \tag{24}$$

Similarly, given $\alpha = 0.8$ and 0.9, we refer to benchmark (24) as CVaR-B-α.

- We also compare the optimal solution of the PPSD problem with the one obtained when no PSPS action is taken, referred to as OrgDS-B.

Recall the earlier discussion on constraint (4): the larger n, the tighter the approximation of the Q-SSD measure. To evaluate the tightness of our Q-SSD model, we pursue a sensitivity analysis by considering four different values of n (i.e., $n = 10, 20, 25,$ and 50), referred to as Q-SSD-n. Fig. 5 illustrates the probability distribution of the random variable C_s^F using different benchmarks. An example to derive the probability distribution of wildfire costs is provided in Appendix A. Compared to OrgDS-B, all (proposed and benchmark) models increase the probabilities of the cases exhibiting low wildfire costs. Within a wildfire cost range between \$3M and \$9M, this probability is the highest when using the VaR-B-α measure. Both Q-SSD-n and CVaR-B-α models reveal higher probabilities than VaR-B-α, when the wildfire cost is lower than \$3M. This indicates that the Q-SSD and CVaR risk measures offer more effective risk mitigation than VaR. According to Fig. 5(a) to (d), an increase in n results in higher probabilities when the wildfire cost is less than \$3M (i.e., 48% for $n = 10$, 56% for $n = 20$, 60% for $n = 25$, and 66% for $n = 50$), highlighting that a tighter approximation of the Q-SSD measure offers a better performance in risk alleviation. One can observe in Fig. 5(d) and (f) that the tightest approximation of the Q-SSD measure performs better than CVaR.

TABLE I
EXPECTED WILDFIRE COSTS, POWER OUTAGE COSTS, AND TOTAL COSTS WITH DIFFERENT BENCHMARK RISK MEASURES

	n	α	Exp. Wildfire Costs ($)	Power Outage Costs ($)	Total Costs ($)
Q-SSD	10	N/A	4,288,702	3,256,928	7,545,630
	20		3,429,951	3,921,452	7,351,403
	25		3,098,408	4,119,458	7,217,866
	50		2,473,985	4,646,512	7,120,497
CVaR	N/A	0.8	3,098,408	4,119,458	7,217,866
		0.9	2,780,541	4,412,652	7,193,193
VaR	N/A	0.8	5,094,272	4,803,560	9,897,832
		0.9	4,902,293	4,946,512	9,848,805

Table I presents the expected wildfire costs, power outage costs, and total costs resulting by Q-SSD-n, CVaR-B-α, and VaR-B-α approaches for different n and α. One can observe that using the VaR-B-α approach results in the largest expected wildfire and power outage costs compared to the costs associated with Q-SSD-n, CVaR-B-α for the given n and α. Compared to CVaR-B-0.9, we can see that Q-SSD-50 decreases the expected wildfire cost by 11% (\$2,473,985 vs. \$2,780,541), while increasing the power outage cost by 5% (\$4,646,512 vs. \$4,412,652). Moreover, the total cost obtained with model Q-SSD-50 is found lower than that with the benchmark model CVaR-B-0.9. Upon analyzing the values of n in the Q-SSD model, one can observe that the proposed Q-SSD model with tighter approximation results in minimal wildfire risk while keeping the severity of PSPS-caused power outages as low as possible.

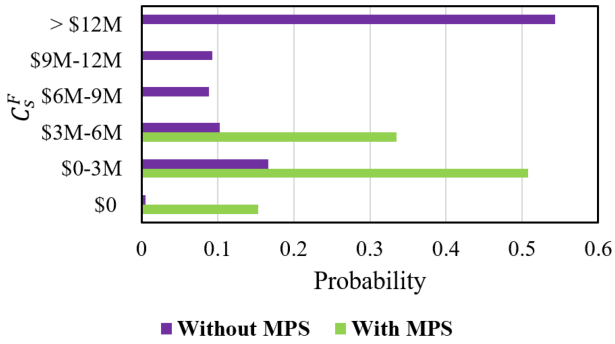

Fig. 6. Probability distribution of different wildfire cost ranges when using the proposed Q-SSD model with and without MPS utilization and dispatch.

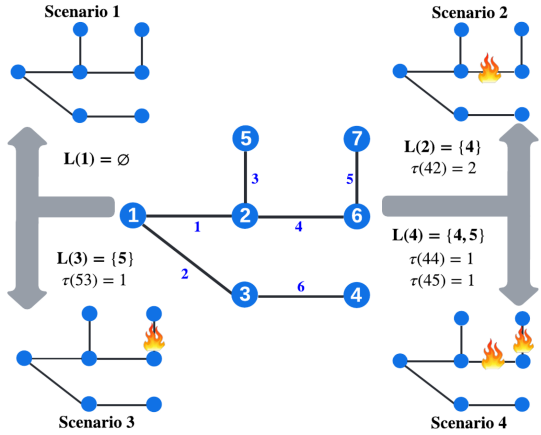

Fig. 7. A simplified DS under different wildfire scenarios.

E. Quantification of MPS Benefits

Fig. 6 illustrates the probability distribution of the random variable C_s^F by solving Q-SSD-50 with and without MPS utilization and dispatch. One can observe that when MPSs are utilized, the higher likelihoods are attributed to the lower range of wildfire costs (e.g., 50% for \$0–3M). In the absence of MPSs, however, higher probabilities are associated with a higher range of wildfire cost (e.g., 54% for >\$12M). Therefore, MPSs provide local energy backup, enabling DS operators to make PSPS decisions more flexibly to reduce the risk of wildfire catastrophes.

V. Conclusion

This article proposed a Q-SSD-based optimization problem to mitigate the risk of electrically-induced wildfires through optimal decisions on proactive power line de-energization and MPSs dispatch. We consider the trade-off between wildfire risk mitigation and minimization of PSPS-caused power outage costs including the revenue loss imposed on the electric utility, the interruption costs imposed to the affected customers, and the operating cost of MPSs which are utilized as backup sources of energy during the PSPS planning horizon. The proposed problem takes the form of an S-MINLP optimization model and captures the uncertainty of wildfire consequences driven by different weather realizations. An efficient linearization method was designed to reformulate the stochastic model into an equivalent MILP formulation. The numerical tests based on the IEEE 33-node test system and the comparison with state-of-the-art benchmark models clearly demonstrate the promising performance of the proposed Q-SSD approach designed for wildfire risk mitigation while keeping the cost of PSPS-caused power outages minimal.

Appendix A
Example for Calculation of C_s^F and the Probability Distribution of the Wildfire Costs

We provide an example to illustrate how to calculate the value of C_s^F based on (8). Consider the DS shown in the center of Fig. A1 with $\mathbf{I} = \{1, \ldots, 7\}$, $\mathbf{L} = \{1, \ldots, 6\}$, $\mathbf{T} = \{1, 2, 3\}$, and $\mathbf{S} = \{1, 2, 3, 4\}$. We consider the following four scenarios:

1) **Scenario 1**: no fault occurs, we directly have $C_1^F = 0$.
2) **Scenario 2**: fault and fire ignition only happen at line 4 at period 2 (i.e., $\tau(42) = 2$):
   - Set $\mathbf{L}(2) = \{4\}$;
   - Sets $\hat{L} = \{4\}$, and $\hat{L}^c = \emptyset$;
   - $C_{\{4\},2} = \$400$.
3) **Scenario 3**: fault and fire ignition only happen at line 5 at period 1 (i.e., $\tau(53) = 1$):
   - Set $\mathbf{L}(3) = \{5\}$;
   - Sets $\hat{L} = \{5\}$, and $\hat{L}^c = \emptyset$;
   - $C_{\{5\},3} = \$100$.
4) **Scenario 4**: fault and fire ignition happen at both lines 4 and 5 at period 1 (i.e., $\tau(44) = \tau(54) = 1$), we have:
   - Set $\mathbf{L}(4) = \{4, 5\}$;
   - Sets *(i)* $\hat{L} = \{4\}$, and $\hat{L}^c = \{5\}$; *(ii)* $\hat{L} = \{5\}$, and $\hat{L}^c = \{6\}$; *(iii)* $\hat{L} = \{4, 5\}$, and $\hat{L}^c = \emptyset$;
   - $C_{\{4\},4} = \$300$, $C_{\{5\},4} = \$200$, and $C_{\{4,5\},4} = \$800$.

Assume now that we have two cases for different PSPS actions: (i) **Case 1**: no PSPS action is taken; (ii) **Case 2**: the only PSPS action taken is to shut off line 5 at period 1 (i.e., $x_{51} = 1$). Below, we show the calculation of C_s^F for every $s \in \mathbf{S}$ in both cases.

1) In **Case 1**:

$$
\begin{aligned}
C_1^F &= 0,\\
C_2^F &= C_{\{4\},2}^F(1 - x_{42}) = 400 \times (1 - 0) = \$400,\\
C_3^F &= C_{\{5\},3}^F(1 - x_{51}) = 100 \times (1 - 0) = \$100,\\
C_4^F &= C_{\{4\},4}^F(1 - x_{41})x_{51} + C_{\{5\},4}^F(1 - x_{51})x_{41}\\
&\quad + C_{\{4,5\},4}^F(1 - x_{41})(1 - x_{51})\\
&= 300 \times (1 - 0) \times 0 + 200 \times (1 - 0) \times 0\\
&\quad + 800 \times (1 - 0) \times (1 - 0) = \$800;
\end{aligned}
$$

2) In **Case 2**:

$$
\begin{aligned}
C_1^F &= 0,\\
C_2^F &= C_{\{4\},2}^F(1 - x_{42}) = 400 \times (1 - 0) = \$400,\\
C_3^F &= C_{\{5\},3}^F(1 - x_{51}) = 100 \times (1 - 1) = 0,
\end{aligned}
$$

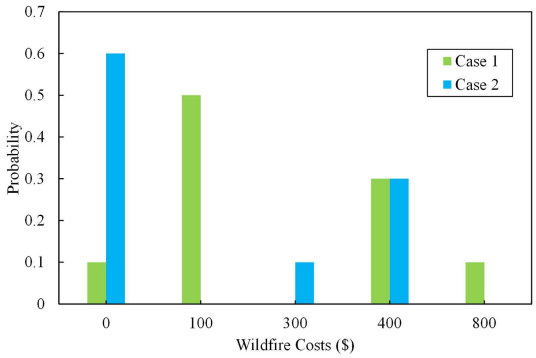

Fig. 8. Probability distribution of the wildfire costs in *Case 1* and *Case 2*.

$$\begin{aligned} C_4^F &= C_{\{4\},4}^F(1-x_{41})x_{51} + C_{\{5\},4}^F(1-x_{51})x_{41} \\ &\quad + C_{\{4,5\},4}^F(1-x_{41})(1-x_{51}) \\ &= 300\times(1-0)\times 1 + 200\times(1-1)\times 0 \\ &\quad + 800\times(1-0)\times(1-1) = \$300. \end{aligned}$$

Next, we depict the calculation of the probability distribution of the wildfire costs under the same setting as in Fig. A1. Assume that the probabilities of the various scenarios are $p_1 = 0.1$, $p_2 = 0.3$, $p_3 = 0.5$, and $p_4 = 0.1$, respectively. Based on the calculated values of C_s^F, the probabilities of wildfire costs in **Case 1** can be obtained:

$$P(0) = 0.1, P(\$400) = 0.3, P(\$100) = 0.5, P(\$800) = 0.1,$$

while the probabilities of wildfire costs in **Case 2** are:

$$P(0) = 0.6, P(\$400) = 0.3, P(\$300) = 0.1.$$

Fig. A2 shows the probability distribution of the wildfire costs obtained in both cases.

Appendix B
Objective Function of Problem PPSD: Properties

Proposition 6: The optimal value of the objective function (15a) is always nonpositive.

Proof: We show that there always exists a feasible solution for which the value of the objective function is zero. The first term $\mathcal{O}$ in the objective function (15a) is equal to 0 when $x_{lt} = 0, l \in \mathbf{L}$ and $t \in \mathbf{T}$, i.e., when no PSPS action is taken. In this case, $CVaR_\alpha(f(x,V)) = CVaR_\alpha(\hat{f}(V)), \alpha \in \mathbf{A}$ which implies that $\max_{\alpha\in\mathbf{A}}(CVaR_\alpha(f(x,V)) - CVaR_\alpha(\hat{f}(V))) = 0$. This provides the result that we set out to prove since not taking any PSPS action is a feasible solution. □

We now propose an alternative formulation

$$\min_{x\in\mathcal{X}} \max_{\alpha\in\mathbf{A}} \left(\mathcal{O} + CVaR_\alpha(f(x,V)) - CVaR_\alpha(\hat{f}(V))\right), \tag{25}$$

for the min-max bi-level objective problem (15a) and show their equivalence in Proposition 7.

Proposition 7: The objective function (15a) can be reformulated as (25).

Proof: Any optimal solutions for problem PPSD minimizes $\mathcal{O}+\mathcal{W} = \mathcal{O}+\max_{\alpha\in\mathbf{A}}(CVaR_\alpha(f(x,V)) - CVaR_\alpha(\hat{f}(V)))$. To prove our statement, we show that for any $x \in \mathcal{X}$, we have $\mathcal{O} + \max_{\alpha\in\mathbf{A}}(CVaR_\alpha(f(x,V)) - CVaR_\alpha(\hat{f}(V))) = \max_{\alpha\in\mathbf{A}}(\mathcal{O} + CVaR_\alpha(f(x,V)) - CVaR_\alpha(\hat{f}(V)))$.
Since, $\mathcal{O}$ does not depend on α, we have $\max_{\alpha\in\mathbf{A}}(\mathcal{O} + CVaR_\alpha(f(x,V)) - CVaR_\alpha(\hat{f}(V))) = \mathcal{O} + \max_{\alpha\in\mathbf{A}}(CVaR_\alpha(f(x,V)) - CVaR_\alpha(\hat{f}(V)))$, and the statement holds. □

We show next in Proposition 8 that one cannot switch the optimization order in (25). In other words, for a given feasible set, the optimization problems $\min_{x\in\mathcal{X}}\max_{\alpha\in\mathbf{A}}$ and $\max_{\alpha\in\mathbf{A}}\min_{x\in\mathcal{X}}$ do not necessarily have the same optimal solution and objective value.

Proposition 8: The optimization problem

$$\max_{\alpha\in\mathbf{A}} \min_{x\in\mathcal{X}} \left(\mathcal{O} + CVaR_\alpha(f(x,V)) - CVaR_\alpha(\hat{f}(V))\right) \tag{26}$$

is not equivalent to problem PPSD.

Proof: Suppose by contradiction that the optimal solution for (26) is optimal for PPSD. Let $\mathcal{O}(x)$ be the value of $\mathcal{O}$ associated with any $x \in \mathcal{X}$. Consider the following example with $\mathbf{A} = \{\alpha_1, \alpha_2\}$, $\mathcal{X} = \{x^1, x^2\}$, $\mathcal{O}(x^1) = 150$, $\mathcal{O}(x^2) = 100$, $CVaR_{\alpha_1}(f(x^1,V)) = 140$, $CVaR_{\alpha_1}(f(x^2,V)) = 200$, $CVaR_{\alpha_2}(f(x^1,V)) = 400$, $CVaR_{\alpha_2}(f(x^2,V)) = 350$, $CVaR_{\alpha_1}(\hat{f}(V)) = 500$, $CVaR_{\alpha_2}(\hat{f}(V)) = 700$. While x^2 is optimal for (15a), it is not the case for (26) for which x^1 is optimal. This proves our statement given that the optimal values of x^1 and x^2 differ. □

While Proposition 8 shows that problems (26) and PPSD do not necessarily have the same optimal value, we notice in our numerical tests that both problems have nonetheless the same optimal value for a number of problem instances.

Appendix C
The Pseudo-Code Description of Algorithm 1

In this Appendix, we present a description of the pseudo-code for Algorithm 1. We use the vocable "Alg-line" to refer to a (numbered) line of the pseudo-code of Algorithm 1. We first initialize some of the sets and indices (Alg-line 1). Next (Alg-lines 2–15), we check one-by-one every pair $(t,l) \in \mathbf{T}\times\mathbf{L}$, and create scenarios depending on how likely it is for line $l \in \mathbf{L}$ to ignite fire during period t. The for-loop for this operation is initiated in Alg-line 2. We first define the extra notation $\hat{s}$ (Alg-line 3) to refer to the last-generated scenario. Next, for any pair (t,l), we go over each scenario $s' \in \{1,\ldots,\hat{s}\}$ to update their probability $p_{s'}$ and to create new scenarios by slightly modifying scenario s' in terms of the status of line l at period t. This is done within the for-loop initiated in Alg-line 4. In Alg-line 5, we check whether line l belongs to set $B(s')$ which includes the lines with fault at period t or earlier under scenario s'. If $l \notin B(s')$, we generate two new scenarios from scenario s'

by changing $\Theta_{ls't}$ from 1 to 0 for those new scenarios (i.e., line l experiencing fault at period t in both new scenarios), and also we update the probability $p_{s'}$ for scenario s' itself. The overhead line l would be considered with a fault at period t if the probability $q_{l,t}^{\text{Fau}}$ is greater than a given threshold ϵ. In Alg-line 6, we test whether $q_{l,t}^{\text{Fau}}$ is greater than ϵ. In Alg-line 7, we find all lines in $\mathbf{L}$ outgoing from line l, and denote this subset of lines by $\tilde{L}(l)$. We generate the two new scenarios in Alg-lines 8 and 9, in which fault on line l is taken into account. The generated scenario in Alg-line 8 has the exact same setting as scenario s', except line l is with fault and ignites fire at period t. The generated scenario in Alg-line 9 is similar to scenario s', except line l is with fault at period t, but does not ignite a fire. In Alg-line 10, we update the probability of scenario s', reducing from $p_{s'}$ to $p_{s'} \times (1 - q_{l,t}^{\text{Fau}})$, considering that line l experiences a fault at period t in the two newly-generated scenarios. We have generated $|\mathbf{S}|$ scenarios up to Alg-line 14. There are some scenarios for which the exact same set of lines ignite a fire at the exact same periods; e.g., suppose for two arbitrary $s', s'' \in \{1, \ldots, s\}$, we have $\mathbf{L}(s') = \mathbf{L}(s'')$ and $\Theta_{ls't} = \Theta_{ls''t}, \forall l \in \mathbf{L}(s')t \in \mathbf{T}$. Based on our definition of set $\mathbf{S}$, each scenario $s \in \mathbf{S}$ must be unique in terms of $\mathbf{L}(s)$ and Θ_{lst} for all $l \in \mathbf{L}(s)t \in \mathbf{T}$. In Alg-lines 15–20, we create a set $\mathbf{S}$ using only such uniquely-generated scenarios. We calculate p_s for every scenario $s \in \mathbf{S}$, $\tau(ls)$, and $l \in \mathbf{L}$ in Alg-lines 21–30.

REFERENCES

[1] J. M. Diaz, "Economic impacts of wildfire," *Southern Fire Exchange*, vol. 498, pp. 2012–2017, 2012.

[2] D. Jones, "October wildfire claims top 9.4 billion statewide," 2017. [Online]. Available: http://www.insurance.ca.gov/0400-news/0100-press-releases/archives/release135-17.cfm

[3] L. A. Hanson, "Wildfire statistics," 2017. [Online]. Available: https://sgp.fas.org/crs/misc/IF10244.pdf

[4] NIFC, "National interagency fire center," 2021. [Online]. Available: https://www.nifc.gov/

[5] S. Jazebi, F. De Leon, and A. Nelson, "Review of wildfire management techniques—Part I: Causes, prevention, detection, suppression, and data analytics," *IEEE Trans. Power Deliv.*, vol. 35, no. 1, pp. 430–439, Feb. 2020.

[6] M. Panteli, C. Pickering, S. Wilkinson, R. Dawson, and P. Mancarella, "Power system resilience to extreme weather: Fragility modeling, probabilistic impact assessment, and adaptation measures," *IEEE Trans. Power Syst.*, vol. 32, no. 5, pp. 3747–3757, Sep. 2017.

[7] S. Jazebi, F. De Leon, and A. Nelson, "Review of wildfire management techniques—Part II: Urgent call for investment in research and development of preventative solutions," *IEEE Trans. Power Del.*, vol. 35, no. 1, pp. 440–450, Feb. 2020.

[8] PG&E Company, "Public safety power shutoff policies and procedures," 2021. [Online]. Available: https://www.pge.com/pge_global/common/pdfs/safety/emergency-preparedness/natural-disaster/wildfires/Public-Safety-Power-Shutoff-Policies-and-Procedures.pdf

[9] D. N. Trakas and N. D. Hatziargyriou, "Optimal distribution system operation for enhancing resilience against wildfires," *IEEE Trans. Power Syst.*, vol. 33, no. 2, pp. 2260–2271, Mar. 2018.

[10] R. Hanna, "Optimal investment in microgrids to mitigate power outages from public safety power shutoffs," in *Proc. IEEE Power Energy Soc. Gen. Meeting*, 2021, pp. 1–5.

[11] PG&E Company, "Pacific gas and electric company amended 2019 wildfire safety plan," 2019. [Online]. Available: https://www.pge.com/pge_global/common/pdfs/safety/emergency-preparedness/natural-disaster/wildfires/Wildfire-Safety-Plan.pdf

[12] G. B. Anderson and M. L. Bell, "Lights out: Impact of the August 2003 power outage on mortality in New York, NY," *Epidemiol. (Cambridge, Mass.)*, vol. 23, no. 2, 2012, Art. no. 189.

[13] C. Zanocco, J. Flora, R. Rajagopal, and H. Boudet, "When the lights go out: Californians' experience with wildfire-related public safety power shutoffs increases intention to adopt solar and storage," *Energy Res. Social Sci.*, vol. 79, 2021, Art. no. 102183.

[14] G. Wong-Parodi, "When climate change adaptation becomes a "looming threat" to society: Exploring views and responses to California wildfires and public safety power shutoffs," *Energy Res. Social Sci.*, vol. 70, 2020, Art. no. 101757.

[15] W. Yang, S. N. Sparrow, M. Ashtine, D. C. Wallom, and T. Morstyn, "Resilient by design: Preventing wildfires and blackouts with microgrids," *Appl. Energy*, vol. 313, 2022, Art. no. 118793.

[16] K. Silverstein, "Microgrids are critical to battle outages caused by wildfires," 2022. [Online]. Available: https://www.environmentalleader.com/2022/02/microgrids-are-critical-to-battle-outages-caused-by-wildfires/

[17] N. Rhodes, L. Ntaimo, and L. Roald, "Balancing wildfire risk and power outages through optimized power shut-offs," *IEEE Trans. Power Syst.*, vol. 36, no. 4, pp. 3118–3128, Jul. 2021.

[18] A. Kody, A. West, and D. K. Molzahn, "Sharing the load: Considering fairness in de-energization scheduling to mitigate wildfire ignition risk using rolling optimization," in *Proc. IEEE 61st Conf. on Decis. and Control*, 2022, pp. 5705–5712.

[19] A. Kody, R. Piansky, and D. K. Molzahn, "Optimizing transmission infrastructure investments to support line de-energization for mitigating wildfire ignition risk," 2022, *arXiv:2203.10176*.

[20] N. Rhodes and L. Roald, "Co-optimization of power line shutoff and restoration for electric grids under high wildfire ignition risk," 2023, *arXiv:2204.02507*.

[21] R. Bayani, M. Waseem, S. D. Manshadi, and H. Davani, "Quantifying the risk of wildfire ignition by power lines under extreme weather conditions," *IEEE Syst. J.*, vol. 17, no. 1, pp. 1024–1034, Mar. 2023.

[22] J. Gorka and L. Roald, "Efficient representations of radiality constraints in optimization of islanding and de-energization in distribution grids," *Electric Power Syst. Res.*, vol. 213, 2022, Art. no. 108578.

[23] A. Lesage-Landry, F. Pellerin, J. A. Taylor, and D. S. Callaway, "Optimally scheduling public safety power shutoffs," *Stochastic Syst.*, early access, Jun. 7, 2023, doi: 10.1287/stsy.2022.004.

[24] R. Bayani and S. D. Manshadi, "Resilient expansion planning of electricity grid under prolonged wildfire risk," *IEEE Trans. Smart Grid*, early access, Jan. 31, 2023, doi: 10.1109/TSG.2023.3241103.

[25] D. Anokhin, P. Dehghanian, M. A. Lejeune, and J. Su, "Mobility-as-a-service for resilience delivery in power distribution systems," *Prod. Oper. Manage.*, vol. 30, no. 8, pp. 2492–2521, 2021.

[26] S. Lei, C. Chen, H. Zhou, and Y. Hou, "Routing and scheduling of mobile power sources for distribution system resilience enhancement," *IEEE Trans. Smart Grid*, vol. 10, no. 5, pp. 5650–5662, Sep. 2019.

[27] J. Su, P. Dehghanian, B. Vergara, and M. H. Kapourchali, "An energy management system for joint operation of small-scale wind turbines and electric thermal storage in isolated microgrids," in *Proc. IEEE North Amer. Power Symp.*, 2021, pp. 1–6.

[28] S. Lei, C. Chen, Y. Li, and Y. Hou, "Resilient disaster recovery logistics of distribution systems: Co-optimize service restoration with repair crew and mobile power source dispatch," *IEEE Trans. Smart Grid*, vol. 10, no. 6, pp. 6187–6202, Nov. 2019.

[29] J. Su, D. Anokhin, P. Dehghanian, and M. A. Lejeune, "On the use of mobile power sources in distribution networks under endogenous uncertainty," *IEEE Trans. Control. Netw. Syst.*, early access, Mar. 13, 2023, doi: 10.1109/TCNS.2023.3256278.

[30] D. Roman, G. Mitra, and V. Zverovich, "Enhanced indexation based on second-order stochastic dominance," *Eur. J. Oper. Res.*, vol. 228, no. 1, pp. 273–281, 2013.

[31] N. Noyan, "Alternate risk measures for emergency medical service system design," *Ann. Oper. Res.*, vol. 181, no. 1, pp. 559–589, 2010.

[32] Y. M. Nie, X. Wu, and T. Homem-de Mello, "Optimal path problems with second-order stochastic dominance constraints," *Netw. Spatial Econ.*, vol. 12, no. 4, pp. 561–587, 2012.

[33] R. Gollmer, U. Gotzes, and R. Schultz, "A note on second-order stochastic dominance constraints induced by mixed-integer linear recourse," *Math. Program.*, vol. 126, no. 1, pp. 179–190, 2011.

[34] D. Dentcheva and A. Ruszczyński, "Portfolio optimization with stochastic dominance constraints," *J. Bank. Finance*, vol. 30, no. 2, pp. 433–451, 2006.

[35] R. T. Rockafellar et al., "Optimization of conditional value-at-risk," *J. Risk*, vol. 2, pp. 21–42, 2000.

[36] R. T. Rockafellar and S. Uryasev, "Conditional value-at-risk for general loss distributions," *J. Bank. Finance*, vol. 26, no. 7, pp. 1443–1471, 2002.

[37] F. Andersson, H. Mausser, D. Rosen, and S. Uryasev, "Credit risk optimization with conditional value-at-risk criterion," *Math. Program.*, vol. 89, no. 2, pp. 273–291, 2001.
[38] N. Noyan and G. Rudolf, "Optimization with multivariate conditional value-at-risk constraints," *Oper. Res.*, vol. 61, no. 4, pp. 990–1013, 2013.
[39] M. E. Baran and F. F. Wu, "Network reconfiguration in distribution systems for loss reduction and load balancing," *IEEE Trans. Power Del.*, vol. 4, no. 2, pp. 1401–1407, Apr. 1989.
[40] D. Coldham, A. Czerwinski, and T. Marxsen, "Probability of bushfire ignition from electric arc faults," HRL Technol. Ltd., Melbourne, VIC, Australia, Tech. Rep. HRL/2010/195, 2011.
[41] Utah Smart Energy Lab, "33-bus distribution system for wildfire arc-ignition analysis," 2020. [Online]. Available: https://usmart.ece.utah.edu/wp-content/uploads/sites/70/2020/12/33bus_wildfire.pdf

Jinshun Su (Graduate Student Member, IEEE) received the B.Eng degree in electrical engineering from the Xi'an University of Technology, Xi'an, China, in 2017, and the M.Sc. degree in electrical engineering from The George Washington University, Washington, DC, USA, in 2019. He is currently working toward the Ph.D. degree in electrical engineering with the Department of Electrical and Computer Engineering, The George Washington University. His research interests include applications of mobile power sources for resilient smart grids, modeling, and analysis of decision-dependent uncertainties in energy system decision making processes.

Saharnaz Mehrani received the Ph.D. degree in business administration, with concentration on operations and information management from the University of Connecticut, Storrs, CT, USA, in 2021. He is currently an Assistant Professor with the Department of Information Technology and Operations Management, Florida Atlantic University, Boca Raton, FL, USA. He was Postdoc with the Department of Electrical and Computer Engineering and Department of Decision Sciences, George Washington University, Washington, DC, USA. His research interests include optimization and data analytics, in both theory and application, to solve deterministic and stochastic optimization problems arising in areas as diverse as healthcare operations management, retail revenue management, logistics and supply chain management, power-system resilience, and risk management.

Payman Dehghanian (Senior Member, IEEE) received the B.Sc. in electrical engineering from the University of Tehran, Tehran, Iran, in 2009, the M.Sc. degree in electrical engineering from the Sharif University of Technology, Tehran, in 2011, and the Ph.D. degree in electrical engineering from Texas A&M University, College Station, TX, USA, in 2017. He is currently an Associate Professor with the Department of Electrical and Computer Engineering, George Washington University, Washington, DC, USA. His research interests include power system reliability, resilience assessment, data-informed decision-making for maintenance, asset management in electrical systems, and smart electricity grid applications. Dr. Dehghanian was the recipient of the 2014 and 2015 IEEE Region 5 Outstanding Professional Achievement Awards, 2015 IEEE-HKN Outstanding Young Professional Award, 2021 Early Career Award from the Washington Academy of Sciences, and 2022 Early Career Researcher Award from George Washington University, Washington.

Miguel A. Lejeune is currently a Professor with the Department of Decision Sciences and has a courtesy appointment with the Department of Electrical and Computer Engineering, George Washington University, Washington, DC, USA. He held visiting positions with Carnegie Mellon University, Pittsburgh, PA, USA, Georgetown University, Washington, University of California, Irvine, Irvine, CA, USA, Naval Postgraduate School, Monterey, CA, and Foundation Getulio Vargas, Rio de Janeiro, Brazil. His research interests includes stochastic programming, distributionally robust optimization, decision-dependent uncertainty, data-driven optimization with applications in finance, supply chain management, and health care and energy. Dr. Lejeune was the recipient of the 2019 Koopman Award of the INFORMS Society, CAREER/Young Investigator Research Grant from the Army Research Office, and IBM Smarter Planet Faculty Innovation Award.